

Semi-Empirical Methods for Coaxial Jet Noise Prediction

O. De Almeida

ISVR Technical Report No 326

September 2008



SCIENTIFIC PUBLICATIONS BY THE ISVR

Technical Reports are published to promote timely dissemination of research results by ISVR personnel. This medium permits more detailed presentation than is usually acceptable for scientific journals. Responsibility for both the content and any opinions expressed rests entirely with the author(s).

Technical Memoranda are produced to enable the early or preliminary release of information by ISVR personnel where such release is deemed to be appropriate. Information contained in these memoranda may be incomplete, or form part of a continuing programme; this should be borne in mind when using or quoting from these documents.

Contract Reports are produced to record the results of scientific work carried out for sponsors, under contract. The ISVR treats these reports as confidential to sponsors and does not make them available for general circulation. Individual sponsors may, however, authorize subsequent release of the material.

COPYRIGHT NOTICE

(c) ISVR University of Southampton All rights reserved.

ISVR authorises you to view and download the Materials at this Web site ("Site") only for your personal, non-commercial use. This authorization is not a transfer of title in the Materials and copies of the Materials and is subject to the following restrictions: 1) you must retain, on all copies of the Materials downloaded, all copyright and other proprietary notices contained in the Materials; 2) you may not modify the Materials in any way or reproduce or publicly display, perform, or distribute or otherwise use them for any public or commercial purpose; and 3) you must not transfer the Materials to any other person unless you give them notice of, and they agree to accept, the obligations arising under these terms and conditions of use. You agree to abide by all additional restrictions displayed on the Site as it may be updated from time to time. This Site, including all Materials, is protected by worldwide copyright laws and treaty provisions. You agree to comply with all copyright laws worldwide in your use of this Site and to prevent any unauthorised copying of the Materials.

UNIVERSITY OF SOUTHAMPTON
INSTITUTE OF SOUND AND VIBRATION RESEARCH
FLUID DYNAMICS AND ACOUSTIC GROUP

Semi-Empirical Methods for Coaxial Jet Noise Prediction

by

Odenir de Almeida

ISVR Technical Report No: 326

September 2008

Authorised for issue by
Professor R J Astley
Group Chairman

© Institute of Sound & Vibration Research

ACKNOWLEDGEMENTS

The author wish to express its appreciation to the following:

Dr. Rod Self and Prof. Dr. Jeremy Astley for the support during the year of 2008 spent in the Institute of Sound and Vibration (ISVR).

CAPES - Coordenação de Aperfeiçoamento de Pessoal de Nível Superior for financial support.

EMBRAER – Empresa Brasileira de Aeronáutica S.A.

CONTENTS

Abstract	vi
Nomenclature.....	vii
List of Figures.....	ix
List of Tables	x
1. INTRODUCTION	1
2. COAXIAL JET FLOW	3
3. REVIEW OF SEMI-EMPIRICAL METHODS	7
3.1. Input Parameters.....	9
3.2. SAE ARP 876D.....	11
3.2.1. Computational Procedure.....	13
3.2.2. Sound Pressure Level Adjustments in Prediction	12
3.3. ESDU 01004.....	20
3.3.1. Computational Procedure.....	21
3.4. SAE AIR 1905 – Method 1 (Rolls-Royce).....	23
3.4.1. Computational Procedure.....	24
3.5. SAE AIR 1905 – Method 2 (Boeing).....	28
3.5.1. Computational Procedure.....	29
3.6. SAE AIR 1905 – Method 3 (NASA).....	35
3.6.1. Computational Procedure.....	38
4. FOUR-SOURCE MODEL	45
4.1. Flow Model.....	45
4.1.1. Isothermal Flow.....	45
4.1.2. Heated Primary Flow	48
4.2. Acoustic Model.....	50

4.2.1. Isothermal Flow.....	50
4.2.2. Heated Primary Flow.....	51
5. NUMERICAL RESULTS.....	56
5.1. Static Condition (observer on ground).....	56
5.2. Isothermal Jet - Coplanar.....	60
5.2.1. General Routines.....	61
5.2.2. Four-Source Method.....	62
5.3. Isothermal Jet – Short-Cowl (3/4 cowl).....	63
5.3.1. General Routines.....	64
5.3.2. Four-Source Method.....	65
5.4. Heated Jet - Coplanar.....	66
5.4.1. General Routines.....	67
5.4.2. Four-Source Method.....	68
5.5. Heated Jet – Short-Cowl (3/4 cowl).....	69
5.5.1. General Routines.....	70
5.5.2. Four-Source Method.....	71
6. CONCLUDING REMARKS.....	72
7. REFERENCES.....	74

Abstract

This work describes and compares the implementation and exploitation of the most common semi-empirical methods for dual-stream (coaxial) jet noise prediction. Six different methods available in the literature were numerically implemented and validated against experimental results. In addition, a detailed discussion is presented in order to show the advantages and disadvantages of each empirical model employed, as well as its limitations.

Special attention is given to the so-called Four-Source model, developed in the Institute of Sound and Vibration (ISVR). This method was carefully examined since it relies on physical assumptions to describe the noise sources inside the coaxial jet flow. Although, it is still an empirical method, its results are found to be more consistent and reliable than the other methods considered.

Nomenclature

D	Jet diameter	[m]
T	Temperature	[K]
V	Velocity	[m/s]
A	Area	[m ²]
θ	Angle from Jet Exit	[°]
P	Pressure	[N/m ²]
f	Frequency	[Hz]
a	Speed of Sound	[m/s]
r	Distance from observer	[m]
SPL	Sound Pressure Level	[dB]
M	Mach Number	
AR	Area Ratio (Secondary:Primary)	
TR (τ)	Temperature Ratio	
TRP	Temperature Ratio (Primary:Ambient)	
TRS	Temperature Ratio (Secondary:Ambient)	
VR (λ)	Velocity Ratio (Secondary:Primary)	
BPR	Bypass Ratio	
St	Strouhal Number	
γ	Specific heat ratio	

Subscripts

e	Effective jet
m	Mixed jet
p	Primary jet
s	Secondary jet
0	Ambient conditions
8	Core nozzle exit location
18	Fan nozzle exit location

List of Figures

Figure 2-1. Variations in Coaxial Jet Configurations: a) Short-cowl; b) $\frac{3}{4}$ cowl; (c) long cowl...3	
Figure 2-2. Initial region of a coaxial jet – taken from reference [6].....5	
Figure 4-1. Characterization of the velocities profile for a coaxial jet.....48	
Figure 5-1. Comparison of data with the prediction – Coplanar (ISO) – General subrotines.61	
Figure 5-2. Comparison of data with the prediction – Coplanar (ISO) – Four-Source.....62	
Figure 5-3. Comparison of data with the prediction – Short-cowl (ISO) – General subrotines. .64	
Figure 5-4. Comparison of data with the prediction – Short-cowl (ISO) – Four-Source.65	
Figure 5-5. Comparison of data with the prediction – Coplanar (HOT) – General subrotines. ..67	
Figure 5-6. Comparison of data with the prediction – Coplanar (HOT) – Four-Source.68	
Figure 5-7. Comparison of data with the prediction – Short-cowl (HOT) – General subrotines.70	
Figure 5-8. Comparison of data with the prediction – Short-cowl (HOT) – Four-Source.71	

List of Tables

Table 3-1. Primary Noise Component – Formulae.....	14
Table 3-2. Secondary Noise Component – Formulae.....	15
Table 3-3. Mixed Noise Component – Formulae.....	16
Table 3-4. Normal Adjustment (DSPL) – Primary Component.....	17
Table 3-5. Normal Adjustment (DSPL) – Secondary Component.....	18
Table 3-6. Normal Adjustment (DSPL) – Mixed Component.....	18
Table 3-7. Acoustic Excitation Adjustment (EX).....	19
Table 3-8. Range of operating conditions covered by the ESDU database.....	21
Table 3-9. Prediction parameters and range of operation.....	35
Table 5-1. Nozzle Geometry.....	57
Table 5-2. Operating conditions – Isothermal and heated flows.....	57
Table 5-3. Description of the observer location in the farfield.....	59
Table 5-4. Standard deviation values – coplanar (ISO) – general subroutines.....	60
Table 5-5. Standard deviation values – coplanar (ISO) – Four Source.....	60
Table 5-6. Standard deviation values – short-cowl (ISO) – general subroutines.....	63
Table 5-7. Standard deviation values – short-cowl (ISO) – Four-Source.....	63
Table 5-8. Standard deviation values – coplanar (HOT) – general subroutines.....	66
Table 5-9. Standard deviation values – coplanar (HOT) – Four-Source.....	66
Table 5-10. Standard deviation values – Short-cowl (HOT) – general subroutines.....	69
Table 5-11. Standard deviation values – Short-cowl (HOT) – Four-Source.....	69

1. INTRODUCTION

The need for reasonably accurate techniques for predicting the noise of coaxial exhaust systems has become a high priority in the aeronautical industry since the introduction of high-bypass turbofan engines. Moreover, with the application of more restrictive limits imposed on aircraft noise as a certification requirement, prediction techniques are needed by the aircraft and engine industries in order to reduce the amount of money spent in doing experimental tests for design selection of components.

Currently, industry relies on database methods (normally from model rig data extrapolated to full scale) and by evolution of past experience to new engine designs. Thus the approach could be summarized as an empirical one that relies heavily on simple scaling laws. As the symmetries underlying scaling laws are removed (e.g. by introduction of azimuthally variations of the flow by the use of chevrons) there is an increasing need for more sophisticated prediction methods.

In the last 30 years numerous efforts have been made by different groups of researchers, to understand the physics of coaxial jets and to develop noise prediction methods. The Society of Automotive Engineers (SAE) has been one of the most active groups working in this area. By the late seventies and beginning of eighties the SAE A-21 committee for aircraft noise decided to issue a document comprising a compilation of methodologies for predicting coaxial jet noise which were in use by Rolls-Royce, NASA-Langley and Boeing (however, it is worth pointing out that those methods failed, to some extent, to match experimental spectra in certain ranges of area and velocities ratios). The document issued – an Airspace Information Report – SAE AIR 1905, was intended to make these methods available to interested parties in industry and elsewhere, who could then judge which was most suitable to their needs.

One of the most recent empirical approaches to deal with the noise prediction of coaxial jets has been devised by Fisher et al. [1],[2] - namely the Four-Source Method. This method relied more on the physics of coaxial jets, trying to separate the source regions inside the flow that contribute to noise generation. Chapter 4 gives a detailed presentation of the Four-Source method.

In summary, the most common standard empirical methods available in the literature for coaxial jet noise prediction are:

- 1) SAE ARP 876D – [3]
- 2) ESDU 01004 – [4]
- 3) SAE AIR 1905 – Method 1 (Rolls-Royce) – [5]
- 4) SAE AIR 1905 – Method 2 (Boeing) – [5]
- 5) SAE AIR 1905 – Method 3 (NASA) – [5]
- 6) FOUR-SOURCE – [1],[2]

This report covers an exploitation of the existing empirical methods for dual-stream (coaxial) jet noise prediction. The main idea is to compare numerical results from such models under different conditions seen experimentally in fly-over and static condition tests. In addition, a detailed commentary is presented in order to show the advantages and disadvantages of each empirical model employed, as well as its limitations.

A numerical description of each empirical model for coaxial jet noise prediction is summarized herein. Additional details should be consulted directly from the references given above.

2. COAXIAL JET FLOW

The introduction of bypass engines, displacing early turbojets, was basically in order to achieve increased thrust and improved economy. However, the so called *turbofan* engine also provided a major amount of jet exhaust noise reduction due to the reduction in the exhaust jet velocity.

Many modern engines have relatively high bypass ratios with the fan jet and the turbine or core jet exhausting through separate coaxial nozzles. Various configurations exist which are often referred to as short, medium, or long cowl engines – Figure 2-1.

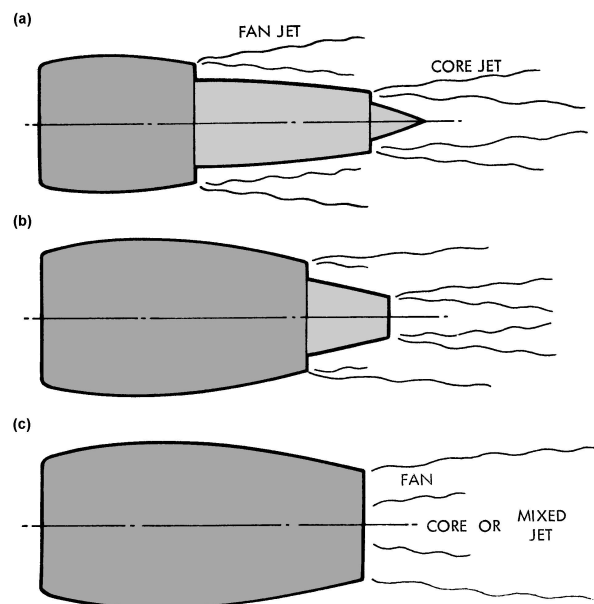


Figure 2-1. Variations in Coaxial Jet Configurations: a) Short-cowl; b) $\frac{3}{4}$ cowl; (c) long cowl.

As can be seen in Figure 2-1 the axial position of the two exhaust nozzles may have influence on the noise from the total jet system. However, this influence is considered to be secondary when compared with the effect of other variable.

The primary variables are:

Area Ratio, $(AR) = \text{Area of bypass nozzle} / \text{Area of core nozzle}$

Velocity Ratio, $(VR) = \text{Velocity of bypass jet} / \text{Velocity of core jet}$

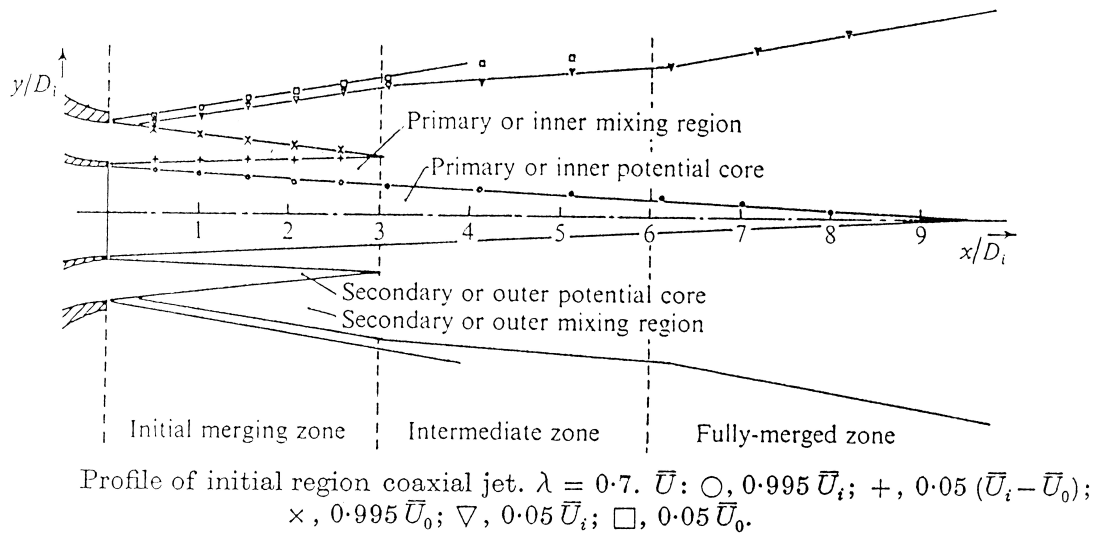
In addition to the variables above, the temperature ratio (TR) is very important, together with a wide range of possible geometric configurations involving the relative positions of the primary and secondary nozzles. A study of the influence of the relative position of the primary and secondary nozzles will be described in Chapter 5.

All these factors or variables, together with a complete understanding of the aerodynamic structure of coaxial jet flow must be taken into consideration in a prediction method for the noise from a coaxial jet. As will be described in the next chapters of this work, this task is not easy and many methods fail to describe or to associate the aerodynamic structure with the generated noise.

From the aerodynamic standpoint, a lot of work has been done in the last few decades on dual-stream flows. However, one of the most referenced articles in this area is that of Ko & Khan [6], which describes a detailed study of the initial region of coaxial jet flows. Doubtless, the most important finding in Ko & Khan's research was the identification of three different zones at different axial positions within the initial jet flow. These zones are depicted in Figure 2-2, originally taken from reference [6].

From the work of [6], it is known that the initial region can be divided into different zones: a) the initial merging; b) intermediate; c) fully-merged zones. The zone which is nearest the nozzle exits and ends roughly at the point where the secondary or outer potential core disappears is called the initial merging zone. The termination of this zone, however, depends on the mean velocity ratio. Immediately downstream from the initial merging zone is the intermediate zone, where the primary potential core still

persists. It is within this zone that mixing of the flows from the two upstream mixing regions occurs. The extent of the intermediate zone is about two to three primary diameters. Finally, the fully-merged zone is the one downstream from the intermediate zone. In this zone the end of the potential core is expected. It is important to say that the extent of the primary potential core depends on the mean-velocity ratio.



\bar{U}_i primary velocity; \bar{U}_0 secondary velocity

Figure 2-2. Initial region of a coaxial jet – taken from reference [6].

The work of Ko & Khan has been utilized by many other researches in this field. As will be described in Chapter 4, an entirely semi-empirical method has been built based on the assumption of zones of separation inside the coaxial flow.

From the acoustic standpoint, several noise source location studies have been performed (e.g Strange et al [7]) supporting the aerodynamic structure proposed by [6]. The work of [6] is also important in this context since the authors identified two different sources inside the coaxial jet, suggesting the existence of two types of vortices at different frequencies. These results allowed the authors to affirm that the higher frequency is found to be generated in the primary or inner mixing region, while the

lower frequencies are generated in the secondary or outer mixing region.

Noise source location, by means of the Polar Correlation technique was performed by [7]. In this work, it was also possible to identify the existence of two spatially distinct source regions inside the coaxial flow for all of the velocity ratios less than one that were tested. These source regions suggest that the higher frequency sound is being emitted by the secondary to ambient shear layer and that the lower frequency sound emerges from the primary to ambient shear layer.

In a general way, the noise from coplanar coaxial jets is more complex than that from a single stream jet. However, it has been identified that the noise is emitted by at least two axially distinct source regions. These consist of a low frequency source at downstream location which is equivalent to the noise from a fully mixed single jet, and a higher frequency region of sound production comprising two characteristically different turbulent volumes, one of which is characterized by the secondary jet conditions and the other by the primary jet velocity.

3. REVIEW OF SEMI-EMPIRICAL METHODS

Generally, jet noise prediction methods are based on a general understanding of the theory and to some extent on research conducted using small scale model nozzles, but primarily on full scale engine tests. Basically, any prediction procedure involves three general steps:

- a. A relationship is developed for jet noise overall sound pressure level (OASPL) at a given radius from the jet engine at a specified angle either from the inlet of the engine or from the exhaust, as a function of jet velocity relative to the ambient air.
- b. A spectrum shape is then predicted in terms of a non-dimensional parameter called the effective Strouhal number. This spectrum is also commonly called the *master-spectra*.
- c. The last step involves the prediction of the OASPL and spectrum shapes at the other angles around the engine.

According to SAE (The Engineering Society for Advancing Mobility Land Sea Air and Space) the activities on the topic of coaxial flow jet mixing noise started in 1974. In 1975, a draft method was proposed by Rolls-Royce, which was based on an adjustment of previous single stream method contained in SAE ARP876 report. The proposal was not accepted due to limitations of the method for matching the experimental database used at that time. In addition, the method failed to cover “inverted velocity profile” exhaust configuration of interest at that time as well, in the context of advanced supersonic transports.

From 1977 to 1983 alternative proposals from Boeing, Rolls-Royce and NASA-Langley were submitted for SAE Aerospace Council approval. However, all of them failed to predict the complete range of experimental configurations tested as a database. Because of the lack of agreement after so many years, in 1983, the Gas Turbine Propulsion Subcommittee decided to issue an AIR (Aerospace Information Report) containing the Rolls Royce, Boeing, and NASA-Langley methods, so as to make them available to interested parties, who could then judge which was appropriate to their needs. It is evident that those methods are unable to cover a complete range of applications either at that time or for modern exhaust engine configurations as seen nowadays.

Besides the methods within the scope of the SAE, another method was being developed almost in parallel. The ESDU (Engineering Sciences Database Unit) prediction routine was developed as part of a parametric study of coaxial jet noise characteristics under the Noise Test Facility at (DERA) RAE, Pyestock – United Kingdom (now the QinetiQ Noise Test Facility). This method has been largely used in the aerospace industry; however, some limitations and flaws have been identified, which exposes again the inability of these methods when applied to specific conditions.

Finally, one of the most recent semi-empirical methods for coaxial jet noise prediction has been reported as the Four-Source method [1],[2]. This method is described completely in the Chapter 4 of this report.

The present chapter is intended to summarize the following methods for coaxial jet noise prediction: a) SAE ARP 876D – [3]; b) ESDU 01004 – [4]; c) SAE AIR 1905 – Method 1 (Rolls-Royce) – [5]; d) SAE AIR 1905 – Method 2 (Boeing) – [5]; e) SAE AIR 1905 – Method 3 (NASA) – [5].

3.1. Input Parameters

For all the empirical methods in this work, the input parameters are quite similar. Basically, they are necessary to describe the ambient conditions, nozzle geometry, nozzle operating conditions and output to a distanced observer. The general input parameters for these methods are:

- Distance from receiver, r [m]
- Angle from engine exhaust axis to receiver, θ [°]
- Ambient static pressure, P_{s0} [Pa]
- Ambient static temperature, T_{s0} [K]
- Flight speed, V_a [m/s]
- Primary jet (core nozzle) static temperature, T_{s8} [K]
- Secondary jet (bypass nozzle) static temperature, T_{s18} [K]
- Core nozzle diameter, D_8 [m]
- Bypass nozzle diameter, D_{18} [m]
- Velocity ratio $\frac{V_{18}}{V_8}$
- Fully expanded primary jet velocity, V_8 [m/s]
- Area ratio $\frac{A_{18}}{A_8}$
- Primary nozzle diameter, D_8 [m]

- Bypass ratio, $BPR = \frac{\dot{m}_{18}}{\dot{m}_8}$

where

$$S_r = \frac{f \cdot D_m}{V_m - V_a} \quad \text{Eq. 3-1}$$

$$D_m = \sqrt{4 \frac{A_8 \cdot \rho_8 \cdot V_8 \cdot (1 + BPR)}{\rho_m \cdot V_m}} \quad \text{Eq. 3-2}$$

$$\rho_m = \frac{P_{s0}}{R \cdot T_{sm}} \quad \text{Eq. 3-3}$$

$$T_{sm} = \frac{T_{s8} + BPR \cdot T_{s18}}{1 + BPR} \quad \text{Eq. 3-4}$$

$$V_m = \frac{V_8 + BPR \cdot V_{18}}{1 + BPR} \quad \text{Eq. 3-5}$$

Some methods require additional parameters, for instance the SAE ARP 876D which needs the following information:

- Fan Rotational Speed, N_1 [RPM]
- $EXA = \frac{\text{distance from fan face to fan duct nozzle}}{\text{fan diameter}}$

In the next sub-sections a synthesis of each aforementioned semi-empirical methods are presented. Essentially, the main purpose of each method is reviewed as well as the numerical procedure to get the sound pressure level predictions. For additional information the listed references should be consulted.

3.2. SAE ARP 876D

The model predicts the noise produced by a subsonic coaxial jet for turbofan engines or scale models. The jet is conceptually divided into three regions; the primary jet, the secondary jet, and the mixed (merged) jet. The method was compiled in 1989, based on parametric correlation of available model databases, independent of other prediction methods and does not require flight corrections.

This jet noise prediction procedure was developed for nozzle area ratio, gas conditions, and aircraft Mach numbers in the following ranges of primary and secondary jet ratios:

$$1.5 < \frac{A_{18}}{A_8} < 3.5 \quad \text{Eq. 3-6}$$

$$2.0 < BPR < 6.5 \quad \text{Eq. 3-7}$$

$$0.6 < \frac{V_{18}}{V_8} < 0.95 \quad \text{Eq. 3-8}$$

$$0.4 < \frac{V_{18}}{a_0} < 1.0 \quad \text{Eq. 3-9}$$

$$0.35 < \frac{T_{T18}}{T_{T8}} < 0.5 \quad \text{Eq. 3-10}$$

$$M_a < 0.3 \quad \text{Eq. 3-11}$$

Moreover, for best accuracy, the frequency range should correspond to a mixed jet Strouhal number:

$$0.1 < S_r < 40 \quad \text{Eq. 3-12}$$

The calculation procedure predicts the one-third octave-band sound pressure level (L) for each component of jet noise at any location. The total jet sound pressure level is $10 \log$ of the sum of the time-mean-square sound pressures from the three

components:

$$L = 10\log(10^{0.1L_p} + 10^{0.1L_s} + 10^{0.1L_m}) \quad \text{Eq. 3-13}$$

where L_p , L_s and L_m are the one-third octave-band sound pressure level of the primary, secondary and mixed jet components, respectively.

Expressions for calculation of jet noise contain three principal groups:

- a. The basic normalized one-third octave-band sound pressure level associated with the shear-layer velocity difference, turbulent eddy convection velocities, and ambient-flow effects;
- b. Normal adjustments to account for effects of ambient air pressure, air density (or temperature), spherical divergence, geometric and acoustic near-field effects, and atmospheric absorption;
- c. Adjustments to account for the effects of internal acoustic excitation.

3.2.1. Sound Pressure Level Adjustments in Prediction

In the SAE ARP 876D prediction method, some adjustments are proposed to the sound pressure levels. They are listed as:

- a. **Normal Adjustments:** For each component-source, the total normal adjustment DSPL is the sum of all the adjustments listed in Table 3-4, Table 3-5 and Table 3-6. The ambient pressure adjustment is the same for all three components. The density effect and spherical divergence are expressed for each component separately.

b. **Near-Field Adjustments:** Empirical adjustments for the separate effects encountered in the acoustic near-field and the geometric near-field were derived from general acoustic and geometric near-field properties. For either acoustic or geometric near-field, the form of adjustment is the same for all three source components – see reference [5].

c. **Atmospheric Attenuation:** The atmospheric attenuation formulas in Table 3-4, Table 3-5 and Table 3-6 include Doppler frequency shift. For flyover noise predictions, the received frequencies have already been Doppler shifted. In a wind tunnel, the locations of the sound sources are stationary and the measured frequencies are the source frequencies. To calculate atmospheric absorption, the measured frequency has to be Doppler shifted and the sound propagation distance through air at rest has to be used.

d. **Acoustic Excitation Adjustments:** Adjustment of the sound pressure level as a result of acoustic excitation in the fan flow is given by the expressions for EX in Table 3-7. As a consequence of the increased mixing rate of an acoustically excited jet, the axial distribution of jet noise sources is more compact than in an unexcited jet.

3.2.2. Computational Procedure

The formulae for each coaxial jet noise components are given in Table 3-1, Table 3-2 and Table 3-3 in sequence. These formulae cover an angular range from 60° to 160°. For locations outside the specified angular range, the limiting angles of 60° and 160° are used in the formulae.

The general equation to compute the sound pressure level at one-third octave band frequency is:

$$SPL = [Z_1 \cdot \log(FV) + Z_2] \cdot [\log S - Z_3 \cdot \log(FV) - Z_4]^2 + Z_5 \cdot \log(FV) + Z_6 \quad \text{Eq. 3-14}$$

Table 3-1. SAE ARP876D - Primary Noise Component – Formulae.

Source Strength Function (FV)	$FV = M_8 \cdot \left(\frac{DVPS}{a_0} \right)^{0.6} \cdot \left(\frac{V_8 + V_{18}}{a_0} \right)^{0.4} \cdot \left(\frac{V_8 - V_a}{V_8} \right)^{n_p}$ $DVPS = \left V_p - \frac{V_a \cdot A_{18} + V_{18} \cdot A_8}{A_{18} + A_8} \right $ <p>if DVPS < 0.3, DVPS = 0.3</p>
Velocity component (n_p)	$n_p = \begin{cases} 1.5 & \theta_p \leq 2.2 \text{ rad} \\ 1.5 \cdot e^{-10 \cdot (\theta_p - 2.2)^2} & \theta_p > 2.2 \text{ rad} \end{cases}$
Strouhal number (S)	$S = \frac{f \cdot D_8}{DVPS}$
Coefficients (Z1)	$Z_1 = -18 \cdot \left[\left(1.8 \frac{\theta_p}{\pi} \right) - 0.6 \right]^2$
(Z2)	$Z_2 = -18 - 18 \cdot \left[\left(1.8 \frac{\theta_p}{\pi} \right) - 0.6 \right]^2$
(Z3)	$Z_3 = 0$
(Z4)	$Z_4 = -0.1 - 0.75 \cdot \left(\frac{V_8 - V_{18} - V_a}{a_0} \right) \cdot \left(1.8 \frac{\theta_p}{\pi} - 0.6 \right)^3 + 0.8 \cdot \left[0.6 - \log \left(1 + \frac{A_{18}}{A_8} \right) \right]$
(Z5)	$Z_5 = 50 + 20 \cdot e^{-(\theta_p - 2.6)^2}$
Z(6)	$Z_6 = 94 + 46 \cdot e^{-(\theta_p - 2.5)^2} - \frac{26 \cdot \left[0.6 - \log \left(1 + \frac{A_{18}}{A_8} \right) \right]}{e^{5(\theta_p - 2.3)^2}} + DSPL + EX$

The procedures for calculating the acoustic excitation adjustment EX and normal adjustment DSPL are reported in [3].

Table 3-2. SAE ARP876D - Secondary Noise Component – Formulae.

Source Strength Function (FV)	$FV = \left(\frac{V_{18} - V_a}{a_0} \right)^{n_s} \cdot \left(\frac{V_{18} + V_a}{a_0} \right)^{1-n_s}$
Velocity component (n_s)	$n_s = 0.5 + 0.1 \cdot \theta_s$
Strouhal number (S)	$S = \frac{f \cdot D_{18}}{V_{18} - V_a}$
Coefficients (Z1)	$Z_1 = -18 \cdot \left[\left(1.8 \frac{\theta_s}{\pi} \right) - 0.6 \right]^2$
(Z2)	$Z_2 = -14 - 8 \cdot \left[\left(1.8 \frac{\theta_s}{\pi} \right) - 0.6 \right]^3$
(Z3)	$Z_3 = -0.7$
(Z4)	$Z_4 = 0.6 - 0.5 \cdot \left(1.8 \frac{\theta_s}{\pi} - 0.6 \right)^2 + 0.5 \cdot \left[0.6 - \log \left(1 + \frac{A_{18}}{A_8} \right) \right]$
(Z5)	$Z_5 = 51 + 54 \cdot \frac{\theta_s}{\pi} - 9 \cdot \left[\left(1.8 \frac{\theta_s}{\pi} \right) - 0.6 \right]^3$
Z(6)	$Z_6 = 99 + 360 \cdot \frac{\theta_s}{\pi} - 15 \cdot \left[\left(1.8 \cdot \frac{\theta_s}{\pi} \right) - 0.6 \right]^4 + 5 \cdot \frac{V_{18} \cdot (V_8 - V_{18})}{a_0^2} + DSPL + EX$

The procedures for calculating the acoustic excitation adjustment EX and normal adjustment DSPL are reported in [3].

Table 3-3. SAE ARP876D - Mixed Noise Component – Formulae.

Source Strength Function (FV)	$FV = \left(\frac{V_m - V_a}{a_0} \right)^{n_m} \cdot \left(\frac{V_m + V_a}{a_0} \right)^{1-n_m}$
Velocity component (n_m)	$n_m = \sqrt{\frac{V_m}{a_0}} \cdot \left[0.6 + \frac{0.2}{0.2 + S_m} \cdot e^{-0.3 \left(\theta_m + \frac{S_m}{1+S_m} - 2.7 \right)^2} \right]$
Strouhal number (S)	$S_m = \frac{f \cdot D_m}{V_m - V_a}$
Coefficients (Z1)	$Z_1 = -30 \cdot \left[\left(1.8 \frac{\theta_m}{\pi} \right) - 0.6 \right]^2$
(Z2)	$Z_2 = -9 - 4 \left(\frac{V_8 - V_{18}}{a_0} \right) - 38 \left[\left(1.8 \frac{\theta_m}{\pi} \right) - 0.6 \right]^3 + 30 \left[0.6 - \log \left(1 + \frac{A_{18}}{A_8} \right) \right] \left(1.8 \frac{\theta_m}{\pi} - 0.6 \right)$
(Z3)	$Z_3 = 1 - 0.4 \cdot \left(1.8 \frac{\theta_m}{\pi} - 0.6 \right)^2$
(Z4)	$Z_4 = 0.44 - \frac{0.5}{e^{\left(4.5 \frac{\theta_m}{\pi} - 4 \right)^2}} + 0.2 \frac{V_8}{a_0} - 0.7 \frac{V_m}{a_0} - 0.2 \log \left(1 + \frac{A_{18}}{A_8} \right) + 0.5 \cdot XBPR \cdot e^{-0.5(\theta_m - 2.4)^2}$ $XBPR = BPR - 5.5 \quad \begin{cases} \text{if } XBPR < 0, XBPR = 0 \\ \text{if } XBPR > 4, XBPR = 4 \end{cases}$
(Z5)	$Z_5 = 34 + 81 \cdot \frac{\theta_m}{\pi} - 20 \cdot \left[\left(1.8 \frac{\theta_m}{\pi} \right) - 0.6 \right]^3$
Z(6)	$Z_6 = 108 + 37.8 \frac{\theta_m}{\pi} + 5 \frac{V_m (V_8 - V_{18})}{a_0^2} - e^{-5(\theta_m - 1.8)^2} + 7 \frac{V_m}{a_0} \frac{\left(1 - 0.4 \frac{V_8}{a_0} e^{-0.7 S_m - 0.8 } \right)}{e^{8(\theta_m - 2.4)^2}} + 0.8 XBPR \cdot e^{\left(\theta_m - 2.3 - \frac{V_m}{a_0} \right)} + DSPL + EX$

The procedures for calculating the acoustic excitation adjustment EX and normal adjustment DSPL are reported in [3].

Normal adjustments to account for effects of ambient air pressure, air density (or temperature), spherical divergence, geometric and acoustic near-field effects, and atmospheric absorption are listed in Table 3-4 for the primary component, Table 3-5 for the secondary component and Table 3-6 for the mixed component respectively.

Table 3-4. SAE ARP876D - Normal Adjustment (DSPL) – Primary Component.

Ambient Pressure	$+ 20\log(P_0 / P_{ISA})$
Density	$+ 20\log\left(\frac{\rho_8 + \rho_{18}}{2\rho_0}\right)$
Spherical Divergence	$+ 20\log(D_8 / r_p)$
Geometric Near-field	$- 10\log\left(1 + \frac{b}{r_p}\right)$ $b = 2D_p + \sqrt{\frac{D_p a_0}{f}}$
Acoustic Near-field	$+ 10\log\left[1 + 0.13\left(\frac{a_0}{r_p f}\right)^2\right]$
Atmospheric Attenuation Coefficient [AC(f)]	$- [AC(f_p)]r_p$ $f_p = \frac{f}{1 - M_0 \cos \theta_p}$

Note: AC(f) is obtained from ARP866A.

Table 3-5. SAE ARP876D - Normal Adjustment (DSPL) – Secondary Component.

Ambient Pressure	$+ 20\log(P_0 / P_{ISA})$
Density	$+ 20\log\left(\frac{\rho_{18} + \rho_0}{2\rho_0}\right)$
Spherical Divergence	$+ 20\log(D_m / r_0)$
Geometric Near-field	$- 10\log\left(1 + \frac{b}{r_s}\right)$ $b = 2D_m + \sqrt{\frac{D_m a_0}{f}}$
Acoustic Near-field	$+ 10\log\left[1 + 0.13\left(\frac{a_0}{r_s f}\right)^2\right]$
Atmospheric Attenuation Coefficient [AC(f)]	$- [AC(f_s)]r_s$ $f_s = \frac{f}{1 - M_0 \cos\theta_s}$

Note: AC(f) is obtained from ARP866A.

Table 3-6. SAE ARP876D - Normal Adjustment (DSPL) – Mixed Component

Ambient Pressure	$+ 20\log(P_0 / P_{ISA})$
Density	$+ 20\log\left(\frac{\rho_m + \rho_0}{2\rho_0}\right)$
Spherical Divergence	$+ 20\log(D_m / r_m)$
Geometric Near-field	$- 10\log\left(1 + \frac{b}{r_m}\right)$ $b = 2D_m + \sqrt{\frac{D_m a_0}{f}}$
Acoustic Near-field	$+ 10\log\left[1 + 0.13\left(\frac{a_0}{r_m f}\right)^2\right]$
Atmospheric Attenuation Coefficient [AC(f)]	$- [AC(f_m)]r_m$ $f_m = \frac{f}{1 - M_0 \cos\theta_m}$

Adjustments to account for the effects of internal acoustic excitation are listed in Table 3-7 for the primary component, secondary and mixed component respectively.

Table 3-7. SAE ARP876D - Acoustic Excitation Adjustment (EX).

Excitation Adjustment (EX)	Primary	Secondary	Mixed
		$EX = 5 \cdot EXD \cdot EXPS$	$EX = \frac{2a_0}{V_{18} \cdot (ZK)}$
Excitation strouhal number S_1	$S_1 = \frac{N_1 D_m}{60 V_m}$		
Effectiveness $EXPS$	$EXPS = e^{-SX}$, where $\begin{cases} SX = 50 \cdot (S_1 - 0.25) \cdot (S_1 - 0.5) \\ SX = 0, \text{ if } 0.25 < S_1 < 0.5, \end{cases}$		
Spectral shape factor EXS	$EXS = 5 \cdot (EXPS) \cdot e^{-\left(\log_{2 \cdot S_1 + 0.00001} \frac{S_m}{2 \cdot S_1 + 0.00001}\right)^2}$ $S_m = \frac{f \cdot D_m}{V_m - V_{18}}$		
Fan duct length factor EXD	$EXD = e^{0.6 - \sqrt{EXA}}$		
Directivity factor EXC	$EXC = \begin{cases} \frac{a_0}{V_m}, & \theta_m \leq 1.4 \\ \frac{a_0}{V_m} \left[1 - \frac{1.8}{\pi} (\theta_m - 1.4) \right], & \theta_m > 1.4 \end{cases}$		
Source location factor ZK	$ZK = 1 - 0.4 \cdot EXD \cdot EXPS$		

Note: $EXA = \text{distance from fan face to fan exit} / \text{Fan diameter}$

3.3. ESDU 01004

ESDU n° 01004, 2001 [4] is a computerized method for estimating exhaust noise spectra from a given database by carrying out a series of interpolations/extrapolations. The computation procedure utilizes two fixed independent variables and the user may select a third independent variable. The fixed independent variables are the normalized primary jet velocity, $\log_{10}(V_p/a_0)$, and the velocity ratio of the secondary to the primary jet flow, (V_s/V_p) .

Data may be input into the database only at values of θ_j that are integer multiples of 10 degrees within the range 0 to 170 degrees. The recommended range of validity for which the method can be used is listed below:

$$\text{Area ratio, } AR = \frac{A_{18}}{A_8} : 1.5 \leq AR \leq 8.0$$

Coplanar exit

$$\text{Strouhal number, } Sr = \frac{f \cdot D_8}{V_8} : -1.5 \leq \log_{10} \left(\frac{f \cdot D_8}{V_8} \right) \leq 1.5$$

The range of operating conditions which the database covers is shown in the following table. Within the table the nominal area ratio values, AR, are listed for different combinations of V_p and V_s/V_p . Actual area ratios were 1.49, 2.02, 4.29 and 7.92.

Table 3-8. Range of operating conditions covered by the ESDU database.

V_s/V_p	AR		
	$V_p = 190 \text{ m/s}$	$V_p = 300 \text{ m/s}$	$V_p = 505 \text{ m/s}$
0	1.5, 2, 4, 8	1.5, 2, 4, 8	1.5, 2, 4, 8
0.2	1.5, 8	1.5, 2, 8	1.5, 2, 4, 8
0.4	1.5, 8	2, 8	1.5, 2, 4, 8
0.6	2, 8	1.5, 2, 8	1.5, 2, 4, 8
0.8	1.5, 2, 8	1.5, 2, 8	–

3.3.1. Computational Procedure

The program normalizes the data for nozzle exit area, radial distance and atmospheric pressure. At the same time, normalization by a term $80 \cdot \log_{10} \left(\frac{V_8}{a_0} \right)$ is also carried out to adjust the data for gross parameter variations and present a “flutter” surface for interpolation/extrapolation. The de-normalization is performed according to the equation 3-15:

$$SPL = SPL_{NORMALIZED} + 10 \cdot \log_{10} \left(\frac{A_8}{r^2} \right) + 20 \cdot \log_{10} \left(\frac{P_{S0}}{P_{ISA}} \right) + 80 \cdot \log_{10} \left(\frac{V_8}{a_0} \right) \quad \text{Eq. 3-15}$$

where $P_{ISA} = 101325 Pa$ in SI units.

3.3.1.1. Interpolation Procedure

For each value of $\log_{10} Sr$, a least-squares fit on the selected database is performed and the resulting regression equation is solved for the jet operating conditions at which the SPL is to be estimated. The optimum combination of terms from the least-squares regression equation, i.e. that which produces the lowest standard error,

is automatically selected for the final regression equation. The option to use two or three independent variables is offered. In both cases the two independent variables, normalized primary jet velocity, $\log_{10}(V_p/a_0)$, and velocity ratio, V_s/V_p , are used. When three independent variables are used the third variable must be selected by the user.

The interpolation procedure is repeated throughout the Strouhal number range of interest for the appropriate angle, θ_j . For values of θ_j that are not integer multiples of 10 degrees, quadratic interpolation using the nearest database angles is carried out. If there are insufficient data for quadratic interpolation, linear interpolation is carried out.

If sufficient data are not available to estimate spectrum values at the edges of the frequency range using the surface-fitting routine, linear extrapolation based on the slope from the two nearest spectral points is carried out, and a warning is printed. The program incorporates a weighting method by which data in the database nearer the point at which spectrum levels are to be estimated are weighted more heavily than data further away.

3.4. SAE AIR 1905 – Method 1 (Rolls-Royce)

The method was developed in 1975, based on modification of single stream method of Appendix A of SAE ARP 876D [5].

The method itself is based on coaxial data where the bypass (fan) flow is cold and the core stream temperature is between 600 and 900 degrees Kelvin.

The correction to the single stream method is a application of a Δ , given by:

$$\Delta = SPL_{COAXIAL} - SPL_{PRIMARY} \quad \text{Eq. 3-16}$$

where Δ is a function of the following principal parameters:

$$\frac{V_8}{a_0} \quad \text{Eq. 3-17}$$

$$\frac{fD_8}{V_8} \quad \text{Eq. 3-18}$$

Area ratio between bypass nozzle and core nozzle, $\frac{A_{18}}{A_8}$

Velocity ratio between bypass exhaust and core exhaust, $\frac{V_{18}}{V_8}$

Angle to intake axis, θ_i

For given T_8 and T_{18} (core and bypass jet temperatures)

3.4.1. Computational Procedure

From V_8 and V_{18} (core and bypass jet velocities), D_8 and D_{18} (core and bypass nozzle diameters) and θ_i (angle to intake axis):

- Δ_m is defined as the mean value of Δ over the range of primary velocities
 $650 \leq V_8 \leq 1250$ (ft/sec)

Then,

$$\Delta_m = f \left\{ \frac{fD_8}{V_8}, AR, VR, \theta_i \right\} \quad \text{Eq. 3-19}$$

- The effect of primary velocity on Δ is accounted for in correlations of Δ' where:

$$\Delta' = 100 \left(\frac{\partial \Delta}{\partial V_8} \right) = f \left\{ \frac{fD_8}{V_8}, AR, VR, \theta_i \right\} \quad \text{Eq. 3-20}$$

- The coaxial correction Δ may be calculated as follows:

$$\Delta = \Delta_m + \Delta' \frac{V_8 - 274}{30.5} \quad \text{Eq. 3-21}$$

Plots of Δ_m against the Strouhal number $\left(\frac{fD_8}{V_8} \right)$ are given in Figures 1-16 of

SAE AIR 1905 [5], for values of θ_i , AR and VR as defined below:

$$\theta_i = 60^\circ, 90^\circ, 120^\circ, 150^\circ$$

$$AR = 1, 2, 4, 6$$

$$VR = 0.2, 0.4, 0.6, 0.8, 1.0$$

Plots of Δ' against the Strouhal number $\left(\frac{fD_8}{V_8}\right)$ are given in Figures 17-19 of

SAE AIR 1905 [5], for values of θ_i , AR and VR as defined below:

$$\theta_i = 60^\circ, 90^\circ, 120^\circ, 150^\circ$$

$$AR = 1, 2, 4, 6$$

$$VR = 1.0 \text{ for } \theta_i = 150^\circ$$

$$VR = 0.6, 0.8, 1.0 \text{ for } 60^\circ \leq \theta_i \leq 120^\circ$$

Where Δ' is not defined, it may be assumed zero.

- The method of calculation is as follows:

Step 1:

Determine: Primary nozzle diameter (D_8)

Secondary nozzle diameter (D_{18})

Primary jet velocity (V_8)

Secondary jet velocity (V_{18})

Primary jet temperature (T_8)

$$\text{Area ratio } AR = \frac{A_{18}}{A_8}$$

$$\text{Velocity ratio } VR = \frac{V_{18}}{V_8}$$

Step 2:

By using Appendix A of ARP876D [3] for single stream jets obtain a plot of the sound pressure level for the primary jet alone at (r, θ_i) in the farfield against 1/3 octave

Strouhal frequencies $\left(\frac{fD_8}{V_8}\right)$.

Step 3:

By using Figures 1-16 – SAE AIR 1905 [5], obtain the 1/3 octave spectrum of Δ_m corresponding to the required angle, area ratio and velocity ratio.

Step 4:

By using Figures 17-19 – SAE AIR 1905 [5], obtain the 1/3 octave spectrum of Δ' corresponding to the required angle, area ratio and velocity ratio.

Step 5:

Compute the spectrum of the coaxial correction Δ by using Δ_m and Δ' from Steps 3 and 4 at corresponding Strouhal frequencies as follows:

$$\Delta = \Delta_m + \Delta' \frac{V_8 - 274}{30.5} \quad \text{Eq. 3-22}$$

Step 6:

Compute the coaxial jet spectrum by adding the coaxial corrections Δ to the primary jet Sound Pressure Levels of Step 2 at corresponding Strouhal frequencies as follows:

$$SPL_{COAXIAL} = SPL_{PRIMARY} + \Delta \quad \text{Eq. 3-23}$$

Step 7:

Obtain the 1/3 octave spectrum levels at position (r, θ_i) and over the range of frequencies from the spectrum of Step 6.

3.5. SAE AIR 1905 – Method 2 (Boeing)

The method (referred as ex-Boeing method) was developed in 1977, based on a 2 source model and completely independent of other prediction methods.

This method considers firstly the normalized overall sound pressure level, OASPL. Then the spectral character, in terms of one-third octave band levels, to the overall level at any point in the field is determined.

The calculation procedure assumes that the following jet flow conditions are available for the primary or inner jet, and the secondary or outer jet;

- a. Fully Expanded Mean Jet Velocities, V_8 and V_{18}
- b. Fully Expanded Mean Jet Density, ρ_8 and ρ_{18}
- c. Mean Total Temperatures, T_{T8} and T_{T18}
- d. Fully Expanded Areas, A_8 and A_{18}

The prediction procedure is restricted to the following range of conditions:

$$1 \leq \frac{A_{18}}{A_8} \leq 6 \quad \text{Eq. 3-24}$$

$$0.4 \leq \frac{V_{18}}{V_8} \leq 2.5 \quad \text{Eq. 3-25}$$

$$0.33 \leq \frac{T_{T18}}{T_{T8}} \leq 3 \quad \text{Eq. 3-26}$$

$$500 \leq V_8 \leq 2000 \text{ ft/s} \quad \text{Eq. 3-27}$$

$$400 \leq V_{18} \leq 2500 \text{ ft/s} \quad \text{Eq. 3-28}$$

$$400 \leq V_m \leq 2000 \text{ ft/s} \quad \text{Eq. 3-29}$$

The prediction procedure is also limited to configurations without a primary centerbody. Thus, the applicability of the method covers:

- a. Coplanar and Retracted primary configurations
- b. Extended primary configuration

3.5.1. Computational Procedure

The method of calculation is described as follows:

Step 1:

Calculate the bypass ratio (BPR)

$$BPR = \frac{\rho_{18} A_{18} V_{18}}{\rho_8 A_8 V_8} \quad \text{Eq. 3-30}$$

Step 2:

Calculate the mixed jet velocity

$$V_m = V_8 \cdot \left[\frac{1 + BPR \left(\frac{V_{18}}{V_8} \right)}{1 + BPR} \right] \quad \text{Eq. 3-31}$$

Step 3:

Calculate the mixed jet total temperature

$$T_{Tm} = T_{T8} \cdot \left[\frac{1 + BPR \left(\frac{T_{T18}}{T_{T8}} \right)}{1 + BPR} \right] \quad \text{Eq. 3-32}$$

Step 4:

Calculate the mixed jet density

$$\rho_m = \frac{P_{S0}}{RT_{SM}} \quad \text{Eq. 3-33}$$

where

$$T_{SM} = T_{TM} - \frac{V_m^2}{2C_p} \quad \text{Eq. 3-34}$$

Step 5:

Calculate the mixed jet area

$$A_m = A_8 \frac{1 + BPR}{\left(\frac{\rho_m}{\rho_8} \right) \left(\frac{V_m}{V_8} \right)} \quad \text{Eq. 3-35}$$

Step 6:

Calculate the mixed jet diameter

$$D_m = \sqrt{\frac{4A_m}{\pi}} \quad \text{Eq. 3-36}$$

Step 7:

With V_m , V_{18} and the ambient speed of sound (a_0) obtain the mixed and secondary jet density exponents (ω_m, ω_{18}) from Figure A.1 of SAE AIR 1905 [5].

Step 8:

For each desired angle and mixed jet velocity, use Figure B.1 of SAE AIR 1905 [5] to obtain the free field normalized overall Sound Pressure Level (S), where:

$$S = OASPL - 10 \cdot \log_{10} \left[\left(\frac{\rho_m}{\rho_0} \right)^{\omega_m} \left(\frac{A_m}{r^2} \right) \left(\frac{T_{Tm}}{T_{T0}} \right)^{m_1} \left(\frac{T_{T0}}{T_{T18}} \right)^{m_2} \right] \quad \text{Eq. 3-37}$$

The mixed jet OASPL temperature-directivity exponents m_1 and m_2 at each angle are given in Figure B.1 of SAE AIR 1905 [5].

Step 9:

Calculate the mixed jet OASPL where:

$$OASPL = S + 10 \cdot \log_{10} \left[\left(\frac{\rho_m}{\rho_0} \right)^{\omega_m} \left(\frac{A_m}{r^2} \right) \left(\frac{T_{Tm}}{T_{T0}} \right)^{m_1} \left(\frac{T_{T0}}{T_{T18}} \right)^{m_2} \right] \quad \text{Eq. 3-38}$$

Step 10:

Determine the mixed jet normalized one-third octave band spectral level by using Figure B.2 of SAE AIR 1905 [5] and

$$Sr = \left(\frac{f \cdot D_m}{V_m} \right) \cdot \frac{1}{\xi_{DF}} \cdot \frac{1}{\xi_{MY}} \quad \text{Eq. 3-39}$$

where the Strouhal connection factors ξ_{DF} ξ_{MY} are obtained from Figure B.3

and B.4 of SAE AIR 1905 [5]. Enter Figure B.2 with the corrected mixed jet Strouhal number to determine:

$$(SPL - OASPL)_m \quad \text{Eq. 3-40}$$

Step 11:

Calculate the mixed jet 1/3 octave band sound pressure level for a given Strouhal number may be determined:

$$SPL_m = OASPL + (SPL - OASPL)_m \quad \text{Eq. 3-41}$$

Step 12:

Correct the mixed jet spectra for the effect of atmospheric attenuation by using ARP 866 procedure.

$$SPL_{m(\text{corrected})} = SPL_m - \frac{\Delta dB}{1000 \text{ ft}} (r - 1) \quad \text{Eq. 3-42}$$

Step 13:

Determine the normalized secondary jet OASPL using Figure B.5 of SAE AIR 1905 [5].

$$S = OASPL - 10 \cdot \log_{10} \left[\left(\frac{\rho_{18}}{\rho_0} \right)^{\omega_{18}} \left(\frac{A_{18}}{r^2} \right) \left(\frac{V_{18}}{V_8} \right)^{-m_4} \right] \quad \text{Eq. 3-43}$$

Step 14:

Calculate the secondary jet OASPL, where

$$OASPL = S + 10 \cdot \log_{10} \left[\left(\frac{\rho_{18}}{\rho_0} \right)^{\omega_{18}} \left(\frac{A_{18}}{r^2} \right) \left(\frac{V_{18}}{V_8} \right)^{-m_4} \right] \quad \text{Eq. 3-44}$$

The secondary jet velocity ratio-directivity exponent m_4 is obtained from

Figure B.6 of SAE AIR 1905 [5].

Step 15:

Calculate the secondary jet peak Strouhal number $(fD_{18}/V_{18})_{PK}$ for each angle, and secondary velocity by using Figure B.7 of SAE AIR 1905 [5].

Step 16:

Calculate the secondary jet normalized one-third octave band spectral levels by using Figure B.8 of SAE AIR 1905 [5] and

$$\frac{\left(\frac{f \cdot D_{18}}{V_{18}}\right)}{\left(\frac{f \cdot D_{18}}{V_{18}}\right)_{PEAK}} \left(\frac{V_{18}}{V_8}\right)^{-m_3} \quad \text{Eq. 3-45}$$

The secondary diameter is that of the outer annulus and is obtained from:

$$D_{18} = \sqrt{\frac{4(A_{18} + A_8)}{\pi}} \quad \text{Eq. 3-46}$$

The velocity ratio-Strouhal connection exponent m_3 is obtained from Figure B.6 of SAE AIR 1905 [5].

Step 17:

The secondary jet 1/3 octave-band SPL is calculated as follows:

$$SPL_{18} = OASPL + (SPL - OASPL)_{18} \quad \text{Eq. 3-47}$$

Step 18:

Correct the secondary jet noise spectra for the effect of atmospheric attenuation using ARP 866.

Step 19:

The total coaxial jet noise 1/3 octave-band SPL is obtained from:

$$SPL = 10 \log_{10} \left(10^{\frac{SPL_{48}}{10}} + 10^{\frac{SPL_m}{10}} \right)$$

Eq. 3-48

Step 20:

Calculate the OASPL for the coaxial jet as follows:

$$OASPL_{Total} = 10 \log_{10} \left(\sum_{m=1}^{m=24 \text{ or } 27} 10^{\frac{SPL_1}{10}} + \dots + 10^{\frac{SPL_n}{10}} \right)$$

Eq. 3-49

Step 21:

Calculate the perceived noise level (PNL) by using ARP 865A.

3.6. SAE AIR 1905 – Method 3 (NASA)

The method (referred as ex-NASA (Langley)) was developed in 1983, based on parametric correlation of available model database, and independent of other prediction methods.

An extensive jet noise data base has been developed from nine separate test series of model data consisting of 214 different circular jet test points and 603 coaxial jet test points from five different industry and government sources. Analysis of the data shows the free field jet mixing noise from subsonic circular jets can be obtained from the jet velocity and jet total temperature. For coaxial jets the free field jet mixing noise with both jets subsonic requires three additional parameters, the jet velocity ratio, the jet total temperature ratio, and the jet area ratio. The prediction parameters and the recommended range of operation for which the method is valid is describe in Table 3-9.

Table 3-9. SAE AIR1905 [5] - Prediction parameters and range of operation.

a. Normalized equivalent jet velocity	$0.3 \leq \frac{V_E}{a_0} \leq 2.0$ $V_E = \frac{\dot{m}_8 \cdot V_8 + \dot{m}_{18} \cdot V_{18}}{\dot{m}_8 + \dot{m}_{18}}$
b. Normalized equivalent jet total temperature	$0.7 \leq \frac{T_{TE}}{T_{s0}} \leq 4.5$ $T_E = \frac{\dot{m}_8 \cdot \left(\frac{\gamma_8}{\gamma_8 - 1} \right) \cdot T_{T8} + \dot{m}_{18} \cdot \left(\frac{\gamma_{18}}{\gamma_{18} - 1} \right) \cdot T_{T18}}{\dot{m}_8 \cdot \left(\frac{\gamma_8}{\gamma_8 - 1} \right) + \dot{m}_{18} \cdot \left(\frac{\gamma_{18}}{\gamma_{18} - 1} \right)}$
c. Velocity ratio	$VR = \frac{V_{18}}{V_8} : 0.02 \leq VR \leq 2.5$
d. Temperature ratio	$TR = \frac{T_{T18}}{T_{T8}} : 0.2 \leq TR \leq 4.0$
e. Area ratio	$AR = \frac{A_{18}}{A_8} : 0.5 \leq AR \leq 10.0$

The free field circular or coaxial jet mixing noise one-third octave band sound pressure level can be expressed in components as:

$$SPL(\theta_i, \eta) = \overline{OAPWL} + DI(\theta_i) + F(\eta) + RSL(\theta_i, \eta) + 20 \cdot \log_{10} \left(\frac{\rho_0 a_0^2}{\rho_{ISA} a_{0-ISA}^2} \right) + 10 \cdot \log_{10} \left(\frac{A_{REF}}{4\pi \cdot r^2} \right) + 197.0 \quad \text{Eq. 3-50}$$

where \overline{OAPWL} is the normalized overall power level, defined by:

$$\overline{OAPWL} = 10 \cdot \log_{10} \left[\frac{\text{Acoustic Power}}{(\dot{m}_{18} + \dot{m}_8) a_0^2} \right] \quad \text{Eq. 3-51}$$

and the reference area is:

$$A_{REF} = \frac{\dot{m}_E}{\rho_0 a_0} \quad \text{Eq. 3-52}$$

It is the area of a cold jet at the critical pressure ratio which has the same mass flow as the hot jet. The mass flow of the equivalent single jet is:

$$\dot{m}_E = \dot{m}_8 + \dot{m}_{18} \quad \text{Eq. 3-53}$$

and r is the distance from the nozzle exit centerline to the observer.

The directivity angle, θ_i , is the angle relative to the inlet axis and the parameter η represents the logarithm of the one-third octave band normalized frequency. The normalized frequency parameter, η , is related to the frequency, f , by

$$\eta = \log_{10} \left(\frac{f \cdot D_e}{V_e} \right) \quad \text{Eq. 3-54}$$

where V_e and D_e are the equivalent jet velocity and jet diameter for a circular or coannular jet.

$DI(\theta_i)$ is the directivity index, calculated as:

$$DI(\theta_i) = \sum_{j=1}^N DI_j(\theta_i) \cdot X_j \quad \text{Eq. 3-55}$$

$F(\eta)$ is the one-third octave band normalized power spectrum, calculated as:

$$F(\eta) = \sum_{j=1}^N F_j(\eta) \cdot X_j \quad \text{Eq. 3-56}$$

$RSL(\theta_i, \eta)$ is the normalized relative spectrum, calculated as:

$$RSL(\theta_i, \eta) = \sum_{j=1}^N RSL_j(\theta_i, \eta) \cdot X_j \quad \text{Eq. 3-57}$$

The overall sound pressure level, OASPL, and the one-third octave band power spectrum level, PWL, can be expressed as:

$$SPL(\theta_i) = \overline{OAPWL} + DI(\theta_i) + 20 \cdot \log_{10} \left(\frac{\rho_0 a_0^2}{\theta_{ISA} a_{0-ISA}^2} \right) + 10 \cdot \log_{10} \left(\frac{A_{REF}}{4\pi \cdot r^2} \right) + 197.0 \quad \text{Eq. 3-58}$$

$$PWL(\eta) = \overline{OAPWL} + F(\eta) + 20 \cdot \log_{10} \left(\frac{\rho_0 a_0^2}{\rho_{ISA} a_{0-ISA}^2} \right) + 10 \cdot \log_{10} \left(\frac{(\dot{m}_8 + \dot{m}_{18}) a_0^2}{\pi_{ref}} \right) + 197.0$$

Eq. 3-59

3.6.1. Computational Procedure

The method of calculation is described in the sequence.

Step 1:

Calculate the equivalent flow properties for the coaxial jet. The single equivalent jet has the same mass flow, enthalpy, and thrust as the coaxial jet. The mass flow of the single equivalent jet is:

$$\dot{m}_E = \dot{m}_8 + \dot{m}_{18} \quad \text{Eq. 3-60}$$

The condition of equivalence of mass flow and thrust gives the equivalent velocity, V_e , as:

$$V_e = \frac{\dot{m}_8 V_8 + \dot{m}_{18} V_{18}}{\dot{m}_8 + \dot{m}_{18}} \quad \text{Eq. 3-61}$$

The equivalent temperature can be defined from the total energy flow as:

$$T_e = \frac{\dot{m}_8 \frac{\gamma_8}{(\gamma_8 - 1)} T_8 + \dot{m}_{18} \frac{\gamma_{18}}{(\gamma_{18} - 1)} T_{18}}{\dot{m}_8 \frac{\gamma_8}{(\gamma_8 - 1)} + \dot{m}_{18} \frac{\gamma_{18}}{(\gamma_{18} - 1)}} \quad \text{Eq. 3-62}$$

where the specific heat ratio, γ , is defined as, $\gamma/(\gamma - 1) = c_p/R$.

The equivalent jet specific ratio is given by:

$$\frac{\gamma_E}{\gamma_E - 1} = \frac{\dot{m}_8 \cdot \left(\frac{\gamma_8}{\gamma_8 - 1} \right) + \dot{m}_{18} \cdot \left(\frac{\gamma_{18}}{\gamma_{18} - 1} \right)}{\dot{m}_8 + \dot{m}_{18}} \quad \text{Eq. 3-63}$$

Because the fully expanded jet static pressure is equal to the ambient pressure the equivalent jet density, ρ_e , can be defined from the ambient jet density, ρ_0 as:

$$\rho_E = \frac{\rho_0}{\left[\frac{T_E}{T_{s0}} - \frac{\gamma_E - 1}{2} \left(\frac{V_E}{a_0} \right)^2 \right]}$$

Eq. 3-64

The equivalent jet area, A_e , is then defined from continuity as:

$$A_E = \frac{\dot{m}_E}{\rho_E V_E}$$

Eq. 3-65

and the equivalent jet diameter, D_e , is:

$$D_E = \sqrt{\frac{4A_E}{\pi}}$$

Eq. 3-66

Also the reference area, A_{ref} , needs to be computed using the expression:

$$A_{REF} = \frac{\dot{m}_E}{\rho_0 a_0}$$

Eq. 3-67

Step 2:

Calculate the parameters x_1 to x_5 from the equivalent jet flow properties and the coaxial jet flow property ratios as follows:

$$x_1 = \log_{10} \left[\frac{V_E}{a_0} \right]$$

Eq. 3-68

$$x_2 = \log_{10} \left[\frac{T_E}{2T_{s0}} \right]$$

Eq. 3-69

$$x_3 = \log_{10} \left[\frac{V_{18}}{V_8} \right]$$

Eq. 3-70

$$x_4 = \log_{10} \left[\frac{T_{T18}}{T_{T8}} \right] \quad \text{Eq. 3-71}$$

$$x_5 = \log_{10} \left[\frac{A_{18}}{A_8} \right] \quad \text{Eq. 3-72}$$

For the circular jet , $V_E = V_8$, $T_E = T_{T8}$ and $x_3 = x_4 = x_5 = 0$.

Step 3:

Using the values of x_1 to x_5 obtained in Step 2 compute the values of the derivative multipliers, X_1 to X_N , as listed in Table C1 of SAE AIR 1905 [5], where N has a value of 8 for the circular jet and a value of 36 for the coannular jet.

Step 4:

Compute the value of the normalized overall power level, \overline{OAPWL} , from the derivative multiplier values, X_j , and the corresponding N number of derivative values, PWL, j , listed in Table C2 of SAE AIR 1905 [5], where N has a value of 8 for the circular jet and a value of 36 for the coannular jet using the relation:

$$\overline{OAPWL} = \sum_{j=1}^N PWL, j X_j \quad \text{Eq. 3-73}$$

Step 5:

Compute the values of directivity index, $DI(\theta_i)$ for θ_j values of 0° , 30° , 60° , 90° , 120° , 150° , and 180° , from the derivative multiplier values, X_j , and the

corresponding N of directivity index derivative values, $DI_{,j}(\theta_i)$, listed in in Table C2 of SAE AIR 1905 [5] using the relation:

$$DI(\theta_i) = \sum_{j=1}^N DI_{,j}(\theta_i) \cdot X_j \quad \text{Eq. 3-74}$$

for $\theta_j = 0^\circ, 30^\circ, 60^\circ, 90^\circ, 120^\circ, 150^\circ, \text{ and } 180^\circ$.

Step 6:

Compute the values of the normalized power spectrum, $F(\eta)$ for η values of -1.5, -1.0, -0.5, 0.0, 0.5, 1.0, and 1.5 from the derivative multiplier values, X_j , and the corresponding number N of power spectrum derivatives values, $F_j(\eta)$ listed in Table C3 of SAE AIR 1905 [5] using the relation:

$$F(\eta) = \sum_{j=1}^N F_j(\eta) \cdot X_j \quad \text{Eq. 3-75}$$

for $\eta = -1.5, -1.0, -0.5, 0.0, 0.5, 1.0, \text{ and } 1.5$.

Step 7:

Compute the values of the normalized relative spectrum, $RSL(\theta_i, \eta)$ for θ_j values of $0^\circ, 30^\circ, 60^\circ, 90^\circ, 120^\circ, 150^\circ, \text{ and } 180^\circ$ and for η values of -1.5, -1.0, -0.5, 0.0, 0.5, 1.0, and 1.5 from the derivative multiplier values, X_j , and the corresponding derivatives values, $RSL_j(\theta_i, \eta)$, in Table C4 of SAE AIR 1905 [5] using the relation:

$$RSL(\theta_i, \eta) = \sum_{j=1}^N RSL_j(\theta_i, \eta) \cdot X_j \quad \text{Eq. 3-76}$$

for $\theta_j = 0^\circ, 30^\circ, 60^\circ, 90^\circ, 120^\circ, 150^\circ,$ and 180° and

for $\eta = -1.5, -1.0, -0.5, 0.0, 0.5, 1.0,$ and $1.5.$

Step 8:

Compute the values of $OASPL(\theta_j)$ for θ_j values of $0^\circ, 30^\circ, 60^\circ, 90^\circ, 120^\circ, 150^\circ,$ and $180^\circ,$ from the value of \overline{OAPWL} obtained in Step 4, the values of $DI(\theta_i)$ obtained in Step 5 and the value of A_{ref} obtained in Step 1, using the equation show below:

$$SPL(\theta_i) = \overline{OAPWL} + DI(\theta_i) + 20 \cdot \log_{10} \left(\frac{\rho_0 a_0^2}{\theta_{ISA} a_{0-ISA}^2} \right) + 10 \cdot \log_{10} \left(\frac{A_{REF}}{4\pi \cdot r^2} \right) + 197.0 \quad \text{Eq. 3-77}$$

Step 9:

Compute the OASPL values at the desired directivity angles (θ_D) by interpolating the OASPL (θ_j) values obtained in Step 8 to obtain the OASPL (θ_D) values using a cubic spline which has zero slope end conditions (directivity angles of 0° and 180°). The cubic spline is a piecewise third order polynomial with continuous slope and curvature at the node points $\theta_j.$

Step 10:

Compute the relative spectrum level values at the desired directivity angles by interpolating the $RSL(\theta_i, \eta)$ values obtained in Step 7 using a cubic spline which has zero slope end conditions for normalized frequency parameter (η) values of $-1.5, -1.0,$

-0.5, 0.0, 0.5, 1.0, and 1.5 to obtain the $RSL(\theta_D, \eta)$ values.

Step 11:

For the desired one third octave band frequencies, (f_D) compute the value of the parameter, η , to obtain the desired η_D values by using the equation as shown:

$$\eta = \log_{10} \left(\frac{f \cdot D_E}{V_E} \right) \quad \text{Eq. 3-78}$$

where f is the desired one third octave band center frequency and V_e and D_e are the equivalent velocity and equivalent diameter computed in Step 1.

Step 12:

Compute the normalized power spectrum levels and the relative spectrum level values at the desired η_D values obtained in Step 11 and the desired directivity angles by interpolating the $F(\eta)$ values obtained in Step 6 and the $RSL(\theta_D, \eta)$ values obtained in Step 10 to obtain the values of $F(\eta_D)$ and the values of $RSL(\theta_D, \eta_D)$ using a cubic spline with zero curvature end conditions ($\eta = -1.5$ and $+1.5$).

Step 13:

Compute the sound pressure level values at the desired directivity angles and desired frequency levels from the values of $F(\eta_D)$ and $RSL(\theta_D, \eta_D)$ obtained in Step 12 and the OASPL (θ_D) values obtained in Step 9 to obtain the values for $SPL(\theta_D, \eta_D)$ using the relation:

$$SPL(\theta_D, \eta_D) = OASPL(\theta_D) + F(\eta_D) + RSL(\theta_D, \eta_D) \quad \text{Eq. 3-79}$$

Step 14:

Also the one third octave band power spectrum level at the desired frequencies can be computed from the \overline{OAPWL} value obtained in Step 4 and the $F(\eta_D)$ values obtained in Step 12 to obtain the values for $PWL(\eta_D)$ using the relation:

$$PWL(\eta) = \overline{OAPWL} + F(\eta) + 20 \cdot \log_{10} \left(\frac{\rho_0 a_0^2}{\rho_{ISA} a_{0-ISA}^2} \right) + 10 \cdot \log_{10} \left(\frac{(\dot{m}_8 + \dot{m}_{18}) a_0^2}{\pi_{ref}} \right) + 197.0$$

Eq. 3-80

4. FOUR-SOURCE MODEL

The essential feature of the four-source model developed for the prediction of the noise from isothermal and heated coaxial jets was the identification of four flow regions whose noise production could be obtained from single stream jet prediction methods.

The description of the Four-Source method is separated in two steps. First, the description of the flow model is important to understand which regions inside the jet plume are contributing to the noise generation. Second, the acoustic model is developed in order to predict the noise spectra for each flow component.

Additional details of the present methodology can be found in the works of [1] and [2].

4.1. Flow Model

4.1.1. Isothermal Flow

A typical flow model for a coaxial jet is shown in Figure 4-1 from which it is possible to identify four potential noise producing regions:

- a. The Primary to Secondary Shear Layer;
- b. Secondary Jet Shear Layer;
- c. The Fully Mixed Jet;
- d. The Interaction Zone

Each one of these four zones is summarized in sequence.

a. The Primary to Secondary Shear Layer

This shear layer separates the initial portions of the primary and secondary flows and has a turbulence level which varies as the difference between the primary and secondary velocities, $(V_p - V_s)$. Hence at velocity ratios of interest for real applications, $\lambda = V_s/V_p \geq 0.5$ the turbulence level is relatively low. Combining this with its relatively small noise producing volume it can be shown that the noise produced in this zone is negligible compared to the other noise producing regions [6]. This flow portion is not considered in the current Four-Source model, however its implementation is very straightforward.

b. Secondary Jet Shear Layer

This shear layer develops between the outer edge of the secondary jet and the ambient fluid. It has the flow characteristics therefore of a jet of diameter equal to that of the secondary jet, D_s , and mean velocity profiles and turbulence levels characteristic of a jet of velocity V_s . However, according to Figure 4-1, this shear layer exists only to the downstream end of the initial merging zone. Its noise production therefore is anticipated to be that of the initial portion of a single jet Diameter D_s , velocity V_s , whose noise production ends when the shear layers merge and enter the intermediate zone.

c. The Fully Mixed Jet

It is well known that the downstream of the coaxial jet development shown in Figure 4-1 the flow becomes that of what is termed a *fully-mixed* jet; that is a jet with

the same mass flow, momentum and energy as that available summing the respective contributions from the primary and secondary jets. Hence on this basis, it is expected the low frequency noise of a coaxial jet to be that of the downstream region of a single jet having the diameter, velocity and temperature of the equivalent fully mixed jet.

d. The Interaction Zone (Effective Jet)

Reference [6] provided vital evidence through a set of turbulence data for a coaxial jet showing that through the interaction region the velocity profiles were characteristic of those of a single jet of velocity V_p and an effective diameter given by:

$$D_e = D_p (1 + \lambda^2 \beta)^{1/2} \quad \text{Eq. 4-1}$$

However a study of the associated turbulence levels indicated that, while these grew from the anticipated levels for the primary and secondary shear layers respectively, the maximum value obtained during merging was only of order 10% of the primary velocity; not 15% as would be anticipated for a single jet. For unheated jet flows, in which only quadrupole radiation is anticipated, allowance for this reduced turbulence level is entirely straightforward. The work of [8] shows that the noise levels vary as the fourth power of the rms turbulence level. Hence a reduction of turbulence level from 15% to 10% will lead to a noise reduction of 7 dB. However, for heated primary flows more care in allowing for this reduced turbulence level is required since both dipole and quadrupole sources contribute.

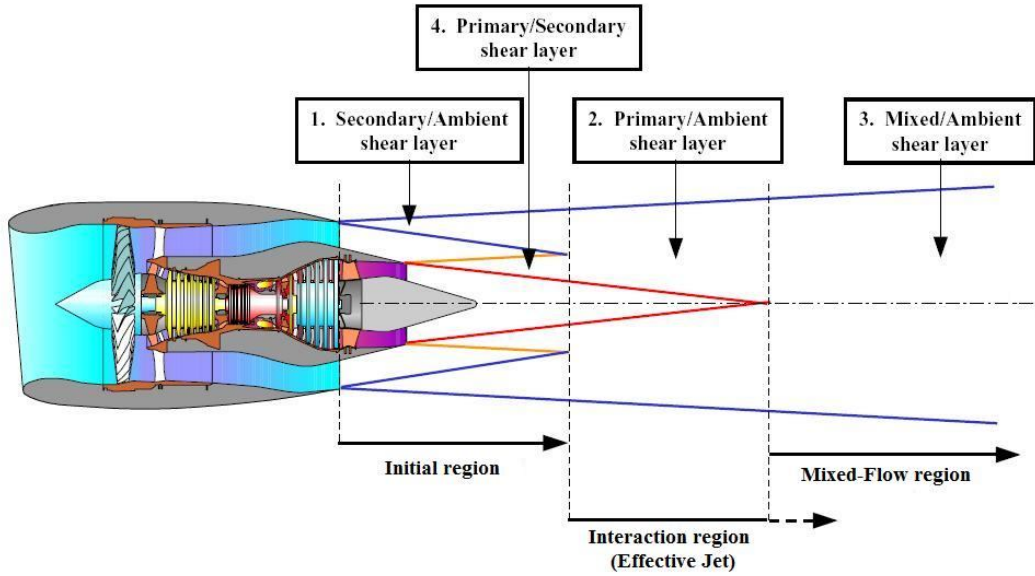


Figure 4-1. Characterization of the velocities profile for a coaxial jet.

4.1.2. Heated Primary Flow

The addition of heat to the primary flow of a coaxial jet introduces a density factor to the conservation of momentum of the whole jet, which can be expressed as:

$$\rho_3 A_3 v_3^2 = \rho_p A_p v_p^2 + \rho_s A_s v_s^2 = \rho_p A_p v_p^2 (1 + \lambda^2 \beta') \quad \text{Eq. 4-2}$$

where $\beta' = A_s \rho_s / A_p \rho_p$.

The secondary jet models the behaviour of the outer shear layer immediately downstream of the nozzle, which is bounded by the unheated secondary flow on its inner boundary and the stationary ambient air at its outer boundary. The temperature of the primary flow therefore has no influence on the sound sources within the secondary shear layer. An identical secondary jet was identified by [9] whose results suggest that it is still a good model for jets with heated primary flow.

The isothermal mixed jet had both the same thrust and mass flow as the coaxial

jet, and may accommodate the hot primary flow by incorporating the modified area ratio β' provided also that it now has the same enthalpy.

Assuming that the heat capacities of the jet exhaust are equal, this may be stated as:

$$T_3(m_1 + m_2) = T_1m_1 + T_2m_2 \quad \text{Eq. 4-3}$$

where mass $m = \rho Av$, or more fully,

$$T_m = \frac{\rho_p A_p v_p T_p + \rho_s A_s v_s T_s}{\rho_p A_p v_p + \rho_s A_s v_s} = T_p \frac{(1 + \lambda \beta' \tau)}{1 + \lambda \beta'} \quad \text{Eq. 4-4}$$

The velocity of the mixed jet is given by substituting β' into Equation (1), but the area is now inextricably linked to the density, the product of which is given by:

$$\rho_m A_m = \rho_p A_p \left(\frac{(1 + \lambda \beta')^2}{1 + \lambda^2 \beta'} \right) \quad \text{Eq. 4-5}$$

However, T_m is known, and since $\rho_p / \rho_m = T_m / T_p$ it can be stated that:

$$A_m = A_p \frac{T_m}{T_p} \left(\frac{(1 + \lambda \beta')^2}{1 + \lambda^2 \beta'} \right) \quad \text{Eq. 4-6}$$

The effective jet is scaled based on the primary jet velocity and so it is reasonable to attribute the same temperature as of the primary flow as well. With regard to the effective jet's diameter it is adopted the same physical dimensions as for the isothermal case. The concept of a turbulent region within the complex coaxial jet structure, which grows in size from the smallest to the largest limit of the jet stream as the velocity ratio varies between zero and one is intuitively sound, and furthermore has been observed for an isothermal coaxial jet, so it seems reasonable to adopt the same physical dimensions for the interaction zone of a heated jet.

4.2. Acoustic Model

The acoustic modelling establishes prediction techniques for each flow region of the coaxial jet flow, as seen previously. A component spectrum is computed for each source zone separately and then summed together to compose the final spectrum for the coaxial jet configuration. In sequence, it will be presented all the formalism for the prediction of unheated and heated flows.

4.2.1. Isothermal Flow

In summary, the isothermal coaxial jet predicted spectrum comprises the following spectral contributions:

a. The high frequencies from a *Secondary Jet*:

$$SPL_s(\theta, f) = SPL(V_s, D_s, \theta, f) + 10 \log_{10} F_U(f_1, f) \quad \text{Eq. 4-7}$$

where $f_1 D_s / U_s = 1$. The factor $F_U(f_1, f)$ represents the cut-off of the spectrum to account for the fact that the noise production from the secondary jet terminates when the primary and secondary shear layers merge; a point at which the width of the secondary shear layer is W_s .

b. The spectrum from an *Effective Jet* whose predicted noise levels are scaled to a 10% turbulence intensity.

$$SPL_e(\theta, f) = SPL(V_p, D_e, \theta, f) + 40 \log_{10} (\alpha / \alpha_0) \quad \text{Eq. 4-8}$$

where, as described previously, $\alpha = 10\%$ and $\alpha_0 = 15\%$. For unheated jets with the 10% turbulence level, the factor $40\log_{10}(\alpha/\alpha_0)$ assumes the constant value of -7 dB correction.

c. The low frequency from a Mixed Jet.

$$SPL_m(\theta, f) = SPL(V_m, D_m, \theta, f) + 10\log_{10} F_D(f_1, f) \quad \text{Eq. 4-9}$$

where $f_1 D_m / U_m = 1$. This expression has the following interpretation. The 1/3 octave sound pressure level contributed by the fully mixed region of the coaxial jet at frequency f and angle θ is given by the sound pressure level predicted for a single jet with velocity V_m and diameter D_m at the corresponding angle and frequency. Because the mixed jet is only relevant downstream of its potential core the predicted spectra are cut-off progressively above the frequency f_1 .

With the three contributions so determined the final prediction is then calculated as the (incoherent) sum of the three components for each 1/3 octave frequency and angle.

4.2.2. Heated Primary Flow

For the prediction of isothermal jets, the high frequency part of the mixed jet's spectrum is cut-off as the secondary jet is being cut-on, in such a way that they are both attenuated by 3 dB at some specified frequency.

It is assumed in changing to a jet with a heated core that the physical structure of the coaxial flow is essentially unchanged, so the extent of the spectral contributions

from the secondary and mixed jets will remain unaltered.

The noise emitted by the effective jet is less than that emitted by a conventional, isolated single jet because of the characteristically reduced turbulence level. It has been argued that the noise emitted by the quadrupole sources of an isothermal jet is proportional to the fourth power of the rms turbulence intensity. However, the noise from the hot effective jet proposed above is the product of both quadrupole and dipole sound sources, so it is necessary to scale the quadrupole noise and the dipole noise separately.

In order to scale the dipole noise correctly it is necessary to find the dependence of far field pressure fluctuations upon the turbulence velocity within the dipole source term, most generally given by:

$$p(\tilde{x}, t) = \frac{-1}{4\pi rc} \frac{x_i}{r} \int_V \frac{\partial F_i}{\partial t} \partial V(\tilde{y}) \quad \text{Eq. 4-10}$$

where F_i is the force per unit volume of each dipole within the source region bounded by the volume V . Reference [10] has shown that the dominant sound radiation from hot jets is associated with the source term as:

$$q = -\frac{\partial}{\partial x_i} \left(\left(\frac{\rho - \rho_0}{\rho} \right) \frac{\partial p}{\partial x_i} \right) \quad \text{Eq. 4-11}$$

Now, it is assumed that all the pressure fluctuations are due to the acceleration of pockets of different density gas, thus equating:

$$\frac{\partial p}{\partial x_i} \text{ with } \rho \frac{\partial U}{\partial t}, \text{ it is possible to rewrite the source term as:}$$

$$q = -\frac{\partial}{\partial x_i} \left((\rho - \rho_0) \frac{\partial U}{\partial t} \right) \quad \text{Eq. 4-12}$$

so, in the farfield:

$$p = \frac{-1}{4\pi r c_0} \frac{x_i}{r} \int_V \frac{\partial}{\partial t} (\rho - \rho_0) \frac{\partial U}{\partial t} \partial V \quad \text{Eq. 4-13}$$

However, $U = U_j + u'$, and U_j is invariant with time so:

$$p = \frac{-1}{4\pi r c_0} \frac{x_i}{r} \int_V \frac{\partial}{\partial t} \left((\rho - \rho_0) \frac{\partial u'}{\partial t} \right) \partial V \quad \text{Eq. 4-14}$$

Now for scaling law purposes, the volume integral can be scaled on a typical dimension D^3 , and assuming a purely Strouhal dependant flow, then the second time derivative scales on the square of frequency or $(U_j / D)^2$, resulting in a farfield pressure:

$$p_{farfield} \propto \frac{(\rho - \rho_0) U_j^2 u' D}{r c_0} \quad \text{Eq. 4-15}$$

The variation of the farfield sound intensity can be expressed as:

$$I \propto \frac{(\rho - \rho_0)^2 U_j^4 u'^2 D^2}{\rho_0 r^2 c_0^3} \quad \text{Eq. 4-16}$$

So, the sound intensity in the farfield due to the dipole sources in a hot turbulent jet is proportional to the square of the rms turbulent velocity. For the effective jet, whose turbulence velocity is characteristically 10% of U_j rather than 15%, the effect will be to reduce the dipole spectrum by an amount:

$$\Delta dB = 20 \log_{10} \left(\frac{10\%}{15\%} \right) = -3.52 dB \quad \text{Eq. 4-17}$$

It remains to determine from the predicted effective jet spectrum how much of the noise is produced by the dipoles and how much by the quadrupole sources, so that each spectrum may be scaled appropriately. To accomplish this task, it is necessary to make use of the theoretical single jet analysis method developed by Szewczyk and

Morfey in 1973 [10]

By applying a geometric acoustic model to the generation of sound by a hot jet, Szewczyk obtained normalized 90° master spectra for quadrupole and volume displacement dipole sources, which when combined with mean flow acoustic interactions form the basis of a single jet prediction program. The advantage of this scheme is that the dipole and quadrupole sources are predicted separately, which enables to reduce the two spectra of the effective jet by 3.5 dB and 7 dB respectively.

The noise reduction is assumed to be:

$$\Delta dB = 10 \log_{10} \left[\frac{r^2 I_d + r^4 I_q}{I_d + I_q} \right] \quad \text{Eq. 4-18}$$

where ΔdB is the reduction, in decibels, applied to the sound pressure level predicted at the third octave band f of the effective jet spectrum, I_d and I_q are the separate far field dipole and quadrupole spectra for the same jet and r is the ratio of turbulence levels, namely $r = (10\% / 15\%)$ as explained previously.

In summary, the hot coaxial jet predicted spectrum comprises the following spectral contributions:

a) The Mixed Jet (low frequencies)

$$SPL_m(\theta, f) = SPL(V_m, T_m, D_m, \theta, f) + 10 \log_{10} F_D(f_1, f) \quad \text{Eq. 4-19}$$

where $f_1 D_m / U_m = 1$.

This equation describes the mixed jet third-octave sound pressure level at an angle θ and frequency f as the sound pressure level predicted for a single jet of

diameter D_m , velocity V_m and temperature T_m at the same angle and frequency, cut-off at frequencies above f_1 as described previously.

b) The Secondary Jet (high frequencies)

$$SPL_s(\theta, f) = SPL(V_s, T_s, D_s, \theta, f) + 10 \log_{10} F_U(f_1, f) \quad \text{Eq. 4-20}$$

where $f_1 D_s / U_s = 1$.

In this case the third-octave sound pressure level from the secondary jet at θ and f is given by the predicted sound pressure level from a jet with the velocity and diameter of the secondary jet at the same angle and frequency, cut-off below the frequency f_1 .

c) The Effective Jet

The spectrum from an effective jet whose predicted noise levels are scaled to a 10% turbulence intensity:

$$SPL_e(\theta, f) = SPL(V_p, T_p, D_e, \theta, f) + \Delta dB \quad \text{Eq. 4-21}$$

The third-octave sound pressure level from the effective jet at θ and f is given by the sound pressure level predicted for a jet at the primary jet velocity and an effective diameter, reduced by a factor which varies between -3.5 dB for a completely dipole-dominated jet to -7 dB for an isothermal jet containing only quadrupoles.

5. NUMERICAL RESULTS

In order to provide a complete basis of comparison for the empirical models, they have been applied to predict farfield jet mixing noise from pure coaxial scale nozzles under stationary conditions (observer on ground). The description of the coaxial nozzles and the operating conditions are given in the next sub-section. The results are shown in sequence for subroutines 1 to 6.

5.1. *Static Condition (observer on ground)*

The numerical results presented in this section are compared against experimental data taken within the EU 6th framework programme CoJeN (Coaxial Jet Noise). A series of jet noise measurements were made, on a scale model basis, with coplanar and short-cowl coaxial nozzles over a range of fully expanded jet velocities compatible with those of aero-engine exhausts. The measurements were made in the geometric far-field where the distributed form of the jet noise source is considered to have negligible effect.

The tests were carried out for a matrix of subsonic jet conditions. The measurements were run at values of V_j/a_0 corresponding to core jet velocities from about 217 m/s to 480 m/s and bypass velocities between 217 m/s and 306 m/s, where V_j is the fully expanded jet velocity and a_0 is the ambient speed of sound. The core jet temperature ratio, defined as the ratio of the jet static temperature (T_{js}) to the ambient temperature (T_0), was set at one of two nominal values, 1.0 (unheated) and 2.6, resulting in a maximum temperature of about 879.9°K. The bypass jet was not heated, e.g an isothermal condition.

For comparison purposes, only two sets of this database have been selected, isothermal cases where both streams are at the same temperature fairly greater than the ambient one, and the heated condition that considers the effect of heating in the primary stream.

Table 5-1 shows the geometry of the nozzles which are used. Table 5-2 describes the test point conditions for isothermal flow (unheated primary flow) as well as a heated primary stream.

Table 5-1. Nozzles Geometry.

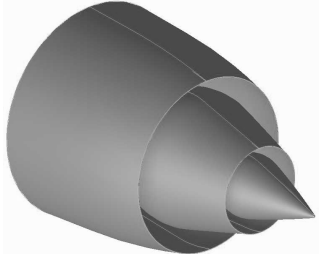
Area Ratio = 3.0, Temperature Ratio = 1.0		
	Velocity Ratio	1.0
	Core Nozzle Diameter (m)	0.095
	Fan Nozzle Diameter (m)	0.200
	Velocity Ratio	1.0
	Core Nozzle Diameter (m)	0.136
	Fan Nozzle Diameter (m)	0.274

Table 5-2. Operating conditions – Isothermal and heated flows.

Condition #	V_p (m/s)	T_{sp} (K)	M_p	T_{tp} (K)	V_s (m/s)	T_{ss} (K)	M_s	T_{ts} (K)	VR
1#Isothermal	217.2	287.58	0.641	311.1	216.8	286.9	0.638	310.2	1.0
2#Heated	480.7	775.6	0.877	879.9	306.8	288.14	0.902	335.0	0.638

Where:

V_p = fully-expanded jet velocity in the primary stream

T_{sp} = static temperature in the primary stream

T_{tp} = total temperature in the primary stream

M_p = Mach number (V_j/a_j) in the primary stream

V_s = fully-expanded jet velocity in the secondary stream

T_{ss} = static temperature in the secondary stream

T_{ts} = total temperature in the secondary stream

M_s = Mach number (V_j/a_j) in the secondary stream

VR = Velocity ratio

The ambient conditions were set according to:

$T_{amb} = 288.14\text{K}$

$a_0 = 340.3 \text{ m/s}$

$P_{amb} = 101.325 \text{ kPa}$

RH = 65.0 %

$\gamma_s = 1.4$

$\gamma_p = 1.35$

Table 5-3 shows the location of the farfield observer as in accordance to the acoustic measurements performed.

Table 5-3. Description of the observer location in the farfield.

Parameter Description	(D) / (θ)
Distance of Receiver [m] / Angle [degrees]	11.74 / 50°
	12.27 / 60°
	12.39 / 70°
	12.64 / 80°
	13.08 / 90°
	13.10 / 100°
	13.21 / 110°
	13.71 / 120°

The subsequent sections will present all the numerical results obtained from the coaxial jet noise prediction routines compared against the experimental results. For better illustration, the results are separated in sections according to the operating conditions and jet geometry. Thus, the sub-sections cover respectively:

- a. Isothermal Jet – Coplanar
- b. Isothermal Jet – Short-cowl
- c. Heated Jet – Coplanar
- d. Heated Jet – Short-cowl

It is important to emphasize, at this point, that most of the methods are devised only for prediction of noise from coplanar coaxial nozzles. There are only two methods available that bring explicitly corrections for extended primary nozzles. They are:

- 1. SAE ARP876D
- 2. SAE AIR1905 – Boeing Method

However, these methods have been applied in industry, at the discretion of engineers, for different types of applications, including short-cowl nozzles. The results herein also include the use of all methods for prediction of noise from short-cowl nozzles.

5.2. Isothermal Jet - Coplanar

A comparison between data and the prediction schemes, here called general subroutines, for isothermal, coplanar nozzles is shown in Figure 5-1. The results from the Four-Source method are shown in Figure 5-2. Both set of spectra were built on a 1/3 octave-band basis.

From Figure 5-1, it is clearly evident that the coaxial jet noise spectra are not fairly reproduced numerically for the angles investigated. The one-third octave spectra are generally over estimated for most of the models, except for the SAE ARP876D method, which appears to under predict the spectra from mid to higher frequencies. The SAE AIR1905-NASA method seems to be closer to the experimental results. In order to have a quantitative parameter of comparison among the methods, the standard deviation from experimental data was calculated. The standard deviation results are in Table 5-4 in sequence, which confirms that the NASA method provides more reasonable results.

Table 5-4. Standard deviation values – coplanar (ISO) – general subroutines.

Method / Angle	50	60	70	80	90	100	110	120
SAE ARP876D	5.27	4.14	3.25	2.94	2.81	3.06	2.93	2.97
ESDU 01004	3.48	3.04	3.84	3.75	3.47	3.45	3.92	4.24
SAE AIR1905 - NASA	1.42	1.54	1.79	1.76	1.55	1.53	2.18	2.55
SAE AIR1905 - Rolls Royce	2.26	1.74	1.78	1.90	2.00	1.96	2.34	2.77
SAE AIR1905 - Boeing	5.54	4.99	4.75	4.46	4.30	3.54	3.55	3.21

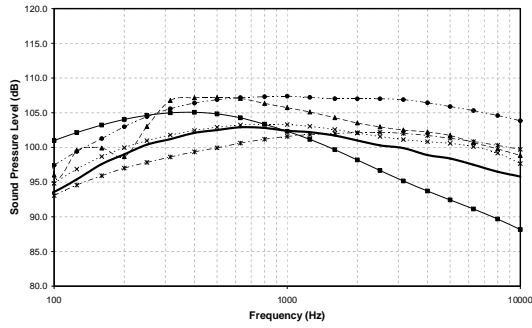
On the other hand, as seen in Figure 5-2, the Four-Source method clearly provided very good results for all the angles investigated. The standard deviation values are presented in Table 5-5, and are less than 0.7 dB for all angles.

Table 5-5. Standard deviation values – coplanar (ISO) – Four Source.

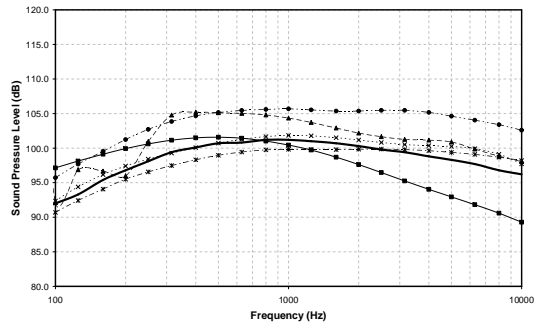
Method / Angle	50	60	70	80	90	100	110	120
FOUR-SOURCE	0.52	0.34	0.47	0.58	0.64	0.47	0.60	0.66

The results show a variation between 1 and 5 decibels for all standard methods. But a very good agreement is seen for the Four-Source method.

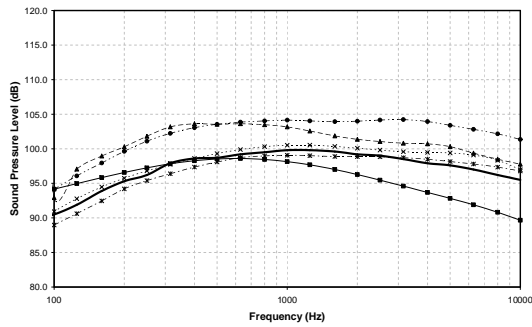
5.2.1. General Routines



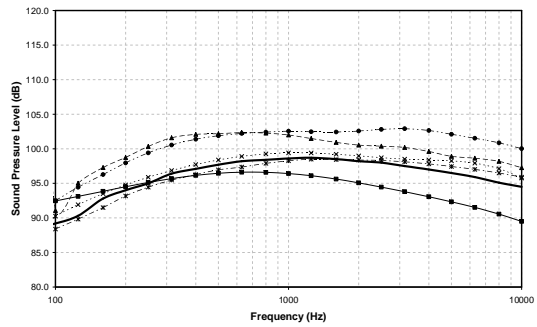
(a) 50°



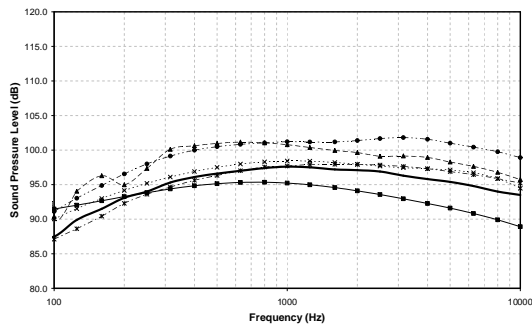
(b) 60°



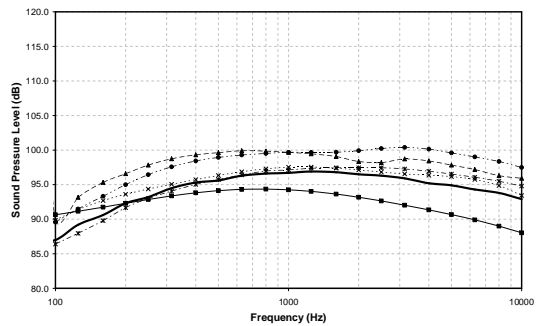
(c) 70°



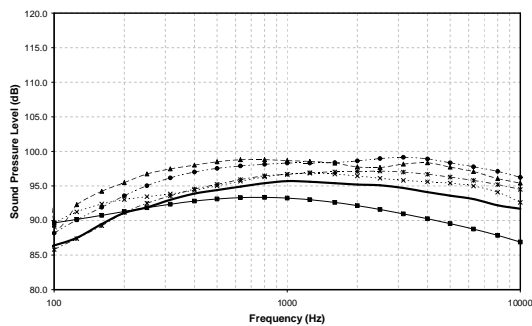
(d) 80°



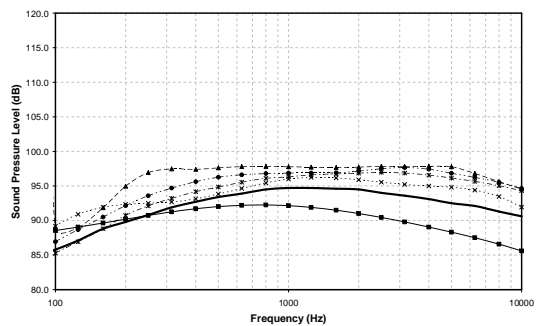
(e) 90°



(f) 100°



(g) 110°

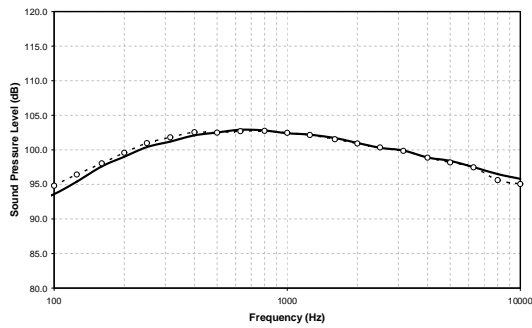


(h) 120°

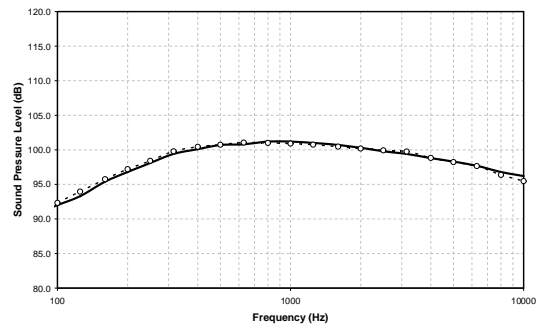
Figure 5-1. Comparison of data with the prediction – Coplanar (ISO) – General subroutines.

— EXP. DATA —■— SAE 876D —▲— ESDU 01004 ---x--- AIR 1905 - NASA —x— AIR 1905 - ROLLS-ROYCE —◆— AIR 1905 - BOEING

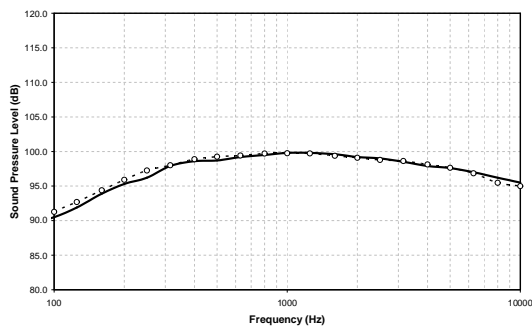
5.2.2. Four-Source Method



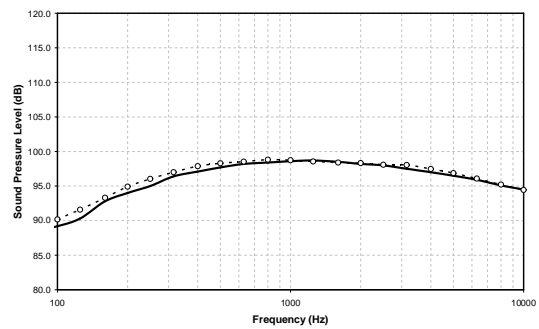
(a) 50°



(b) 60°



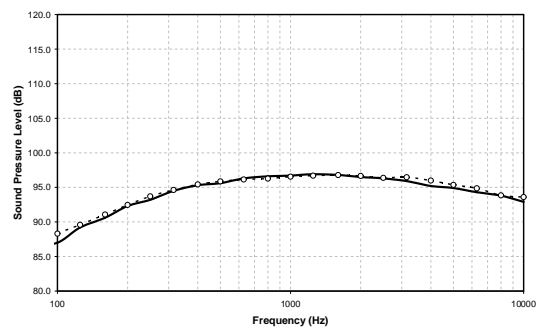
(c) 70°



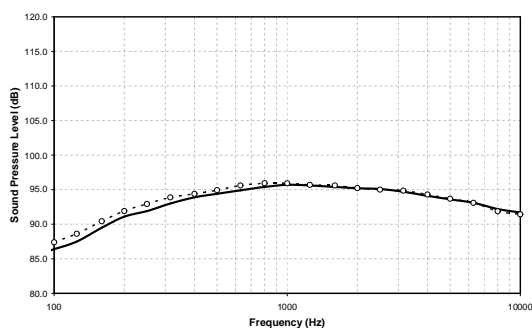
(d) 80°



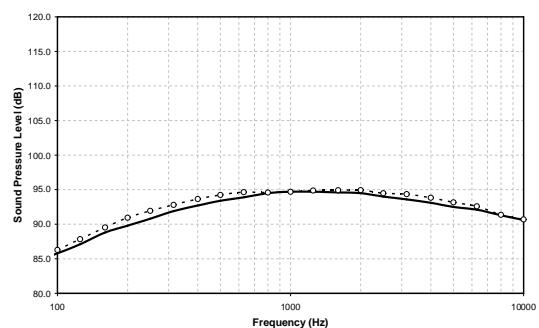
(e) 90°



(f) 100°



(g) 110°



(h) 120°

Figure 5-2. Comparison of data with the prediction – Coplanar (ISO) – Four-Source.

5.3. Isothermal Jet – Short-Cowl (3/4 cowl)

Despite the fact that many of the methods in this study are not devised to predict the noise from short-cowl nozzle configurations, they have been used in this work. The results are shown in Figure 5-3. The results from the Four-Source method are presented in Figure 5-4.

A very similar trend to the coplanar coaxial jet is observed, although some sharper discrepancies are revealed for the ESDU method at the low and high frequency extremities of the spectra. This behaviour was attributed to the extrapolation approach that applies in the database for the current method.

Again, as a quantitative parameter, the standard deviation values are presented in Table 5-6 and Table 5-7 for the general subroutines and the Four-Source method, respectively.

Table 5-6. Standard deviation values – short-cowl (ISO) – general subroutines.

Method / Angle	50	60	70	80	90	100	110	120
SAE ARP876D	5.56	4.70	4.04	3.68	3.23	3.25	2.99	2.97
ESDU 01004	3.97	4.28	4.34	3.93	4.05	3.96	4.45	5.13
SAE AIR1905 - NASA	1.36	1.45	1.69	1.73	1.56	1.60	2.11	2.62
SAE AIR1905 - Rolls Royce	1.77	1.67	1.72	1.68	1.52	1.45	1.86	2.54
SAE AIR1905 - Boeing	4.60	3.61	3.31	3.30	3.44	2.99	3.08	3.00

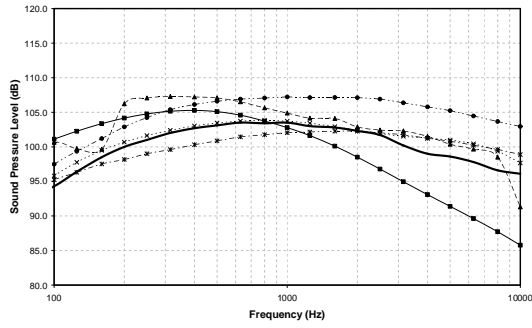
Both NASA and Rolls-Royce methods provided reasonable results all over the angles, the first going better for angles below 80° and the second going well for angles above 80°.

As expected, the Four-Source predictions were poorer than the coplanar ones, since there is no correction for short-cowl nozzles. However, the results seems to be much better when compared to traditional methods.

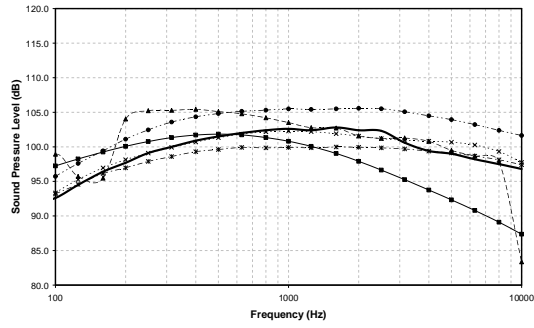
Table 5-7. Standard deviation values – short-cowl (ISO) – Four-Source.

Method / Angle	50	60	70	80	90	100	110	120
FOUR-SOURCE	0.64	0.97	1.07	0.83	0.72	0.73	1.00	1.20

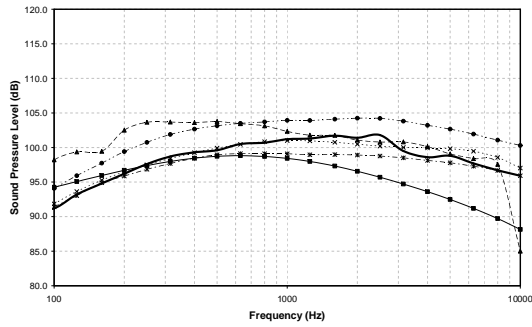
5.3.1. General Routines



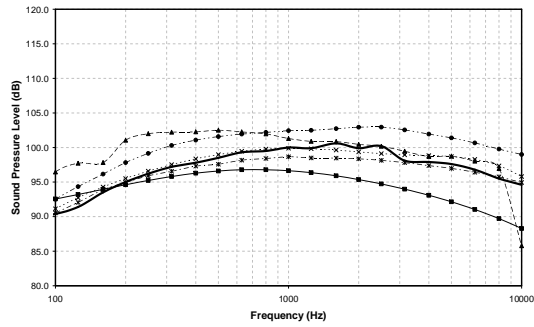
(a) 50°



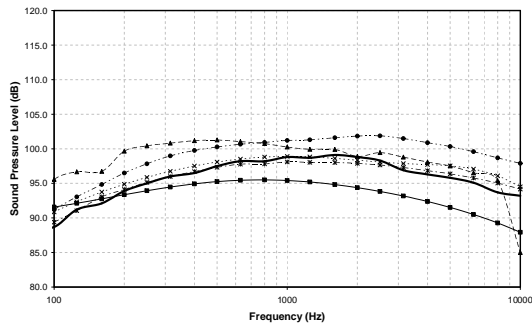
(b) 60°



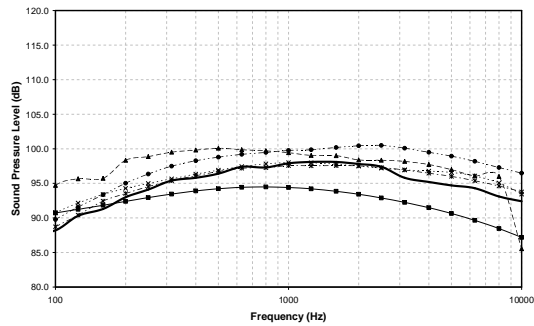
(c) 70°



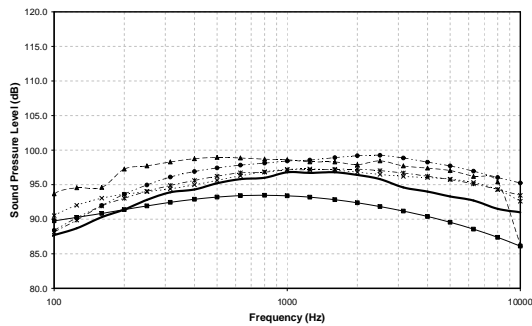
(d) 80°



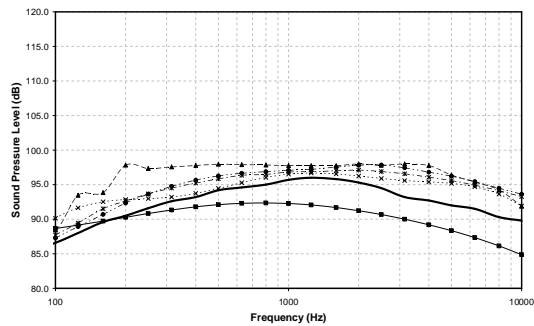
(e) 90°



(f) 100°



(g) 110°

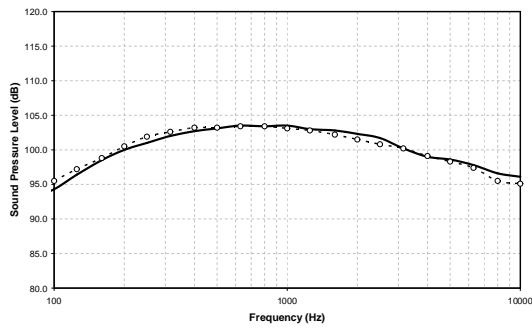


(h) 120°

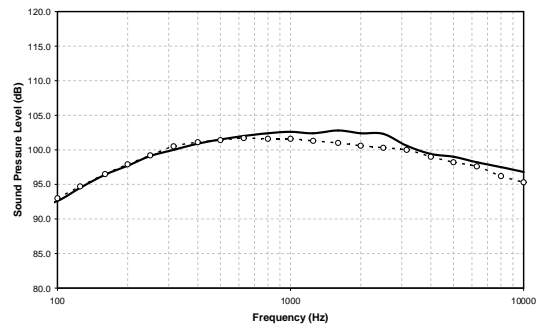
Figure 5-3. Comparison of data with the prediction – Short-cowl (ISO) – General subrotines.

— EXP. DATA —■— SAE 876D —▲— ESDU 01004 ---x--- AIR 1905 - NASA —x— AIR 1905 - ROLLS-ROYCE --●-- AIR 1905 - BOEING

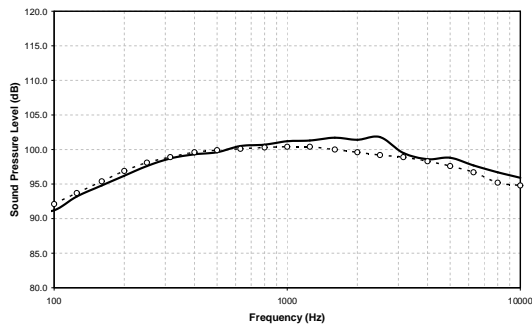
5.3.2. Four-Source Method



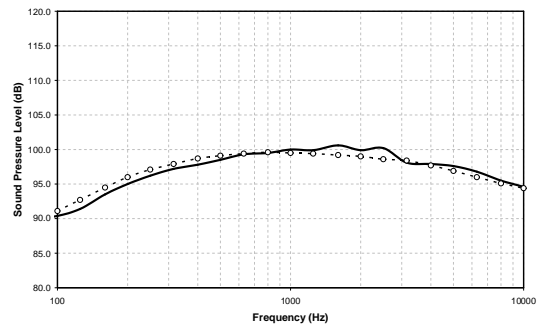
(a) 50°



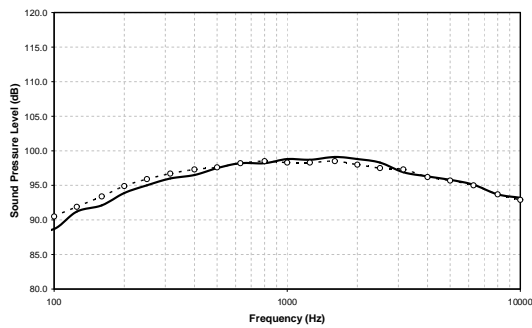
(b) 60°



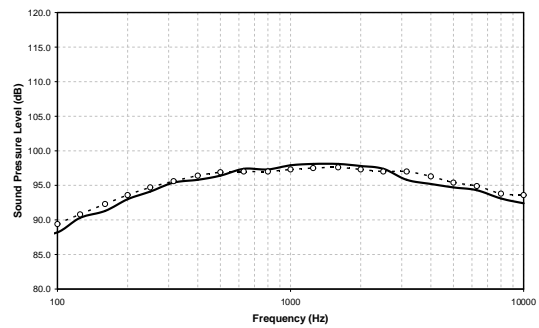
(c) 70°



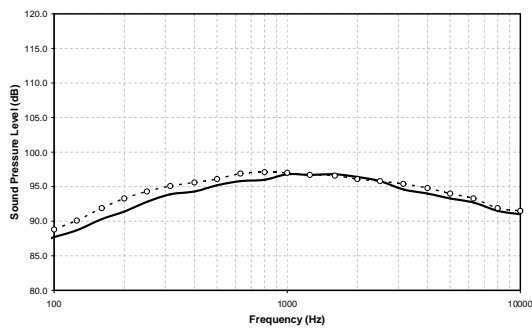
(d) 80°



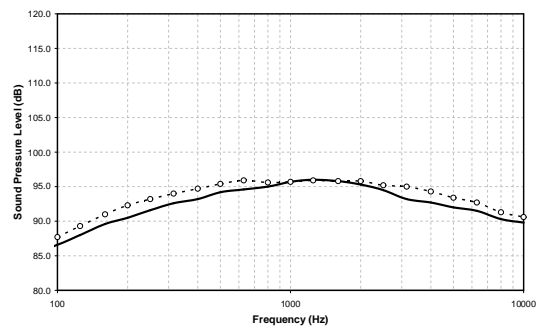
(e) 90°



(f) 100°



(g) 110°



(h) 120°

Figure 5-4. Comparison of data with the prediction – Short-cowl (ISO) – Four-Source.

5.4. Heated Jet - Coplanar

The spectra from a heated, coplanar coaxial jet are shown in Figure 5-5 and Figure 5-6, for the general subroutines and the Four-Source method, respectively.

Reasonable results are observed at mid to low frequencies in the spectrum, for almost all angles. However, big discrepancies are observed in the high frequency range. The NASA and Boeing methods failed to predict the fall-off in the spectrum at frequencies above 1000 Hz. The ESDU method again presents peaks at the low extremity of the spectra for all angles, which supports the idea of misinterpolation on the database. Nevertheless, for frequencies above 200 Hz, the ESDU method presented a good agreement for the spectra, including the high frequency content, at all angles. To be consistent with this fact, for the standard deviation values calculation, in Table 5-8, the ESDU points below 200 Hz have been removed. So, except for low frequency misleading by the ESDU method, it seems to provide the best fit when compared against any other method.

Table 5-8. Standard deviation values – coplanar (HOT) – general subroutines.

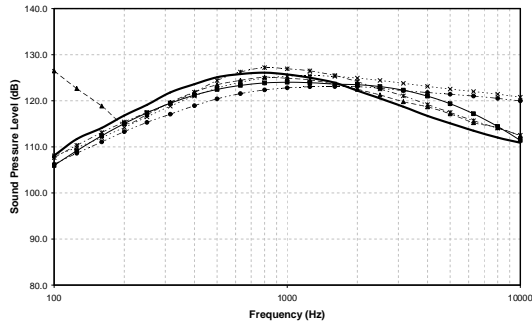
Method / Angle	50	60	70	80	90	100	110	120
SAE ARP876D	2.91	2.48	2.27	2.73	2.96	3.20	3.55	4.26
ESDU 01004	1.52	1.54	1.70	1.76	1.83	1.69	1.87	2.67
SAE AIR1905 - NASA	4.54	3.62	3.38	2.88	2.97	4.05	4.35	5.45
SAE AIR1905 - Rolls Royce	1.68	1.51	1.85	1.63	2.16	2.47	2.63	2.60
SAE AIR1905 - Boeing	4.49	2.48	2.73	2.44	2.97	3.06	3.28	3.49

Table 5-9 shows the standard deviation values for the Four-Source method. The results corroborate the fact that the method was not good for the high frequency part of the spectra, with an overprediction of sound levels. This was more pronounced for angles above 80°. However, all the results are less than 3 dB error.

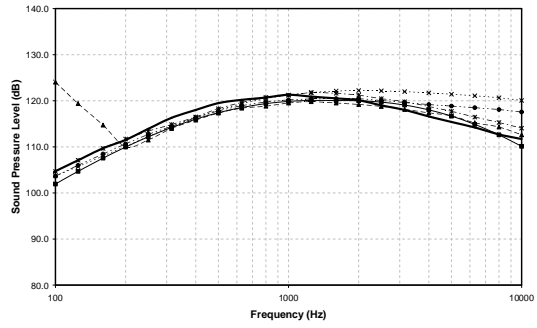
Table 5-9. Standard deviation values – coplanar (HOT) – Four-Source.

Method / Angle	50	60	70	80	90	100	110	120
FOUR-SOURCE	0.96	1.05	1.89	2.47	2.49	2.67	2.65	2.95

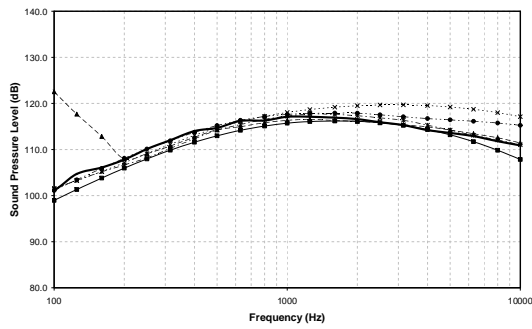
5.4.1. General Routines



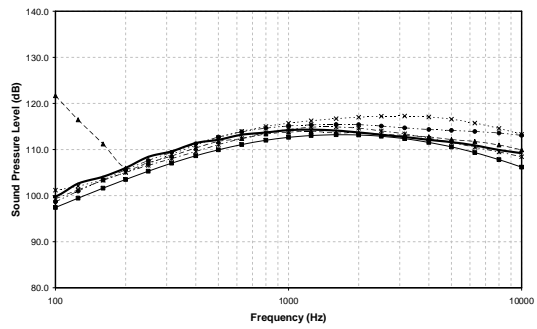
(a) 50°



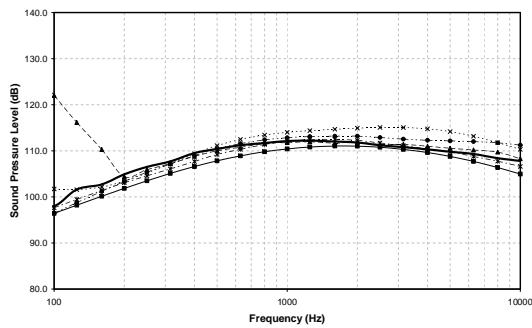
(b) 60°



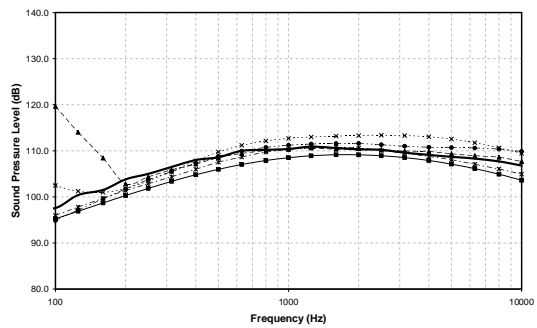
(c) 70°



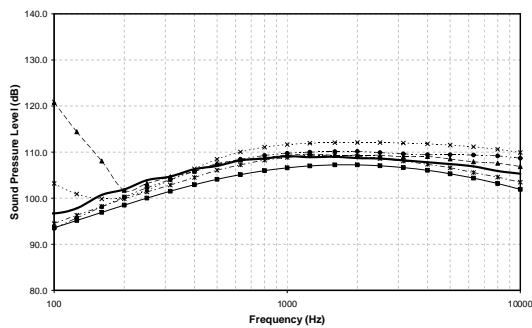
(d) 80°



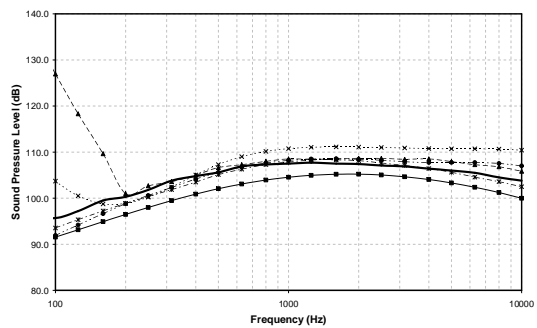
(e) 90°



(f) 100°



(g) 110°

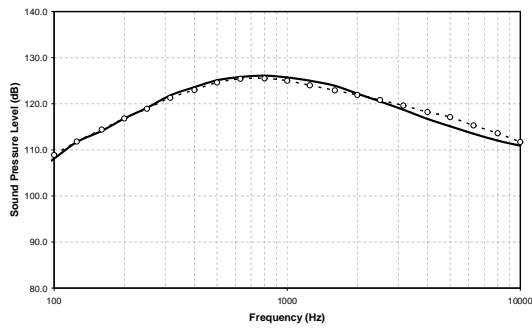


(h) 120°

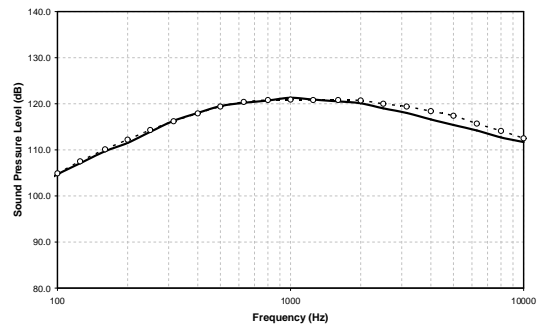
Figure 5-5. Comparison of data with the prediction – Coplanar (HOT) – General subrotines.

— EXP. DATA —■— SAE 876D —▲— ESDU 01004 ---x--- AIR 1905 - NASA —x— AIR 1905 - ROLLS-ROYCE --♦-- AIR 1905 - BOEING

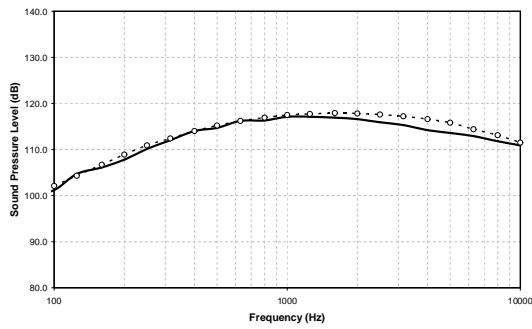
5.4.2. Four-Source Method



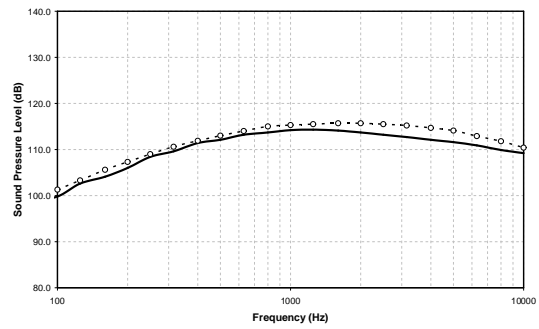
(a) 50°



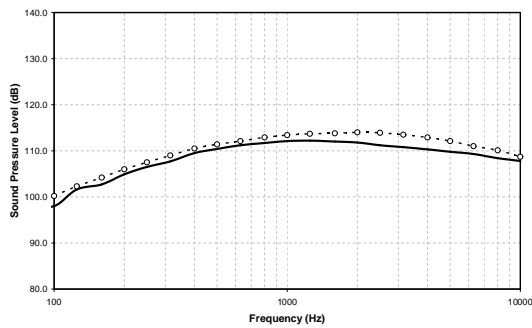
(b) 60°



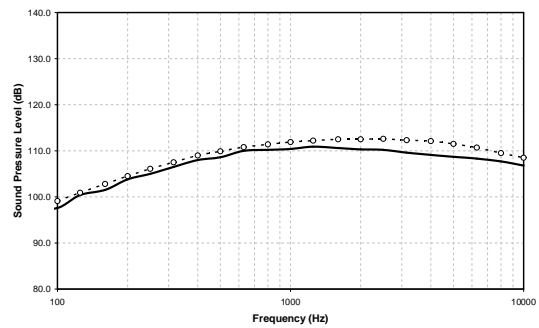
(c) 70°



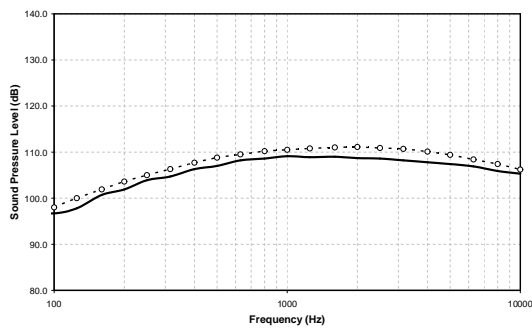
(d) 80°



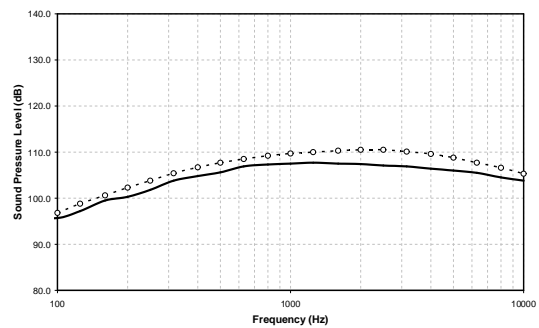
(e) 90°



(f) 100°



(g) 110°



(h) 120°

Figure 5-6. Comparison of data with the prediction – Coplanar (HOT) – Four-Source.

5.5. Heated Jet – Short-Cowl (3/4 cowl)

Finally, the results for a heated, short-cowl nozzle jet are presented in Figure 5-7 and Figure 5-8, for the general subroutines and the Four-Source method, respectively.

As seen previously, the trend in the results are quite similar of those for heated, coplanar jet. In fact, since the nozzles have roughly the same dimensions and are operating at the same conditions, plus the fact that no corrections were applied to the short-cowl, the results should be consistently similar. It is important to notice that, although corrections were present for SAE ARP876D and AIR 1905 (Boeing method), the final results are not the best ones. It is worth saying that those corrections are quite simple and do not include effects like the presence of the plug.

Table 5-10 and Table 5-11 present the standard deviation values for the noise prediction routines. Again, for the ESDU method, the points below 200 Hz were discarded. However, even after excluding these points, the method was not particular effective in predicting the noise levels. The Rolls-Royce method gave the reasonable prediction at this time. **Table 5-10. Standard deviation values – Short-cowl (HOT) – general subroutines.**

Method / Angle	50	60	70	80	90	100	110	120
SAE ARP876D	1.93	1.31	2.15	2.48	2.27	2.45	2.75	3.48
ESDU 01004	2.51	2.57	2.83	2.78	2.90	2.56	2.86	3.57
SAE AIR1905 - NASA	4.44	3.72	3.47	2.89	2.83	3.79	3.98	4.95
SAE AIR1905 - Rolls Royce	1.33	1.43	1.33	1.95	2.02	2.37	2.58	2.65
SAE AIR1905 - Boeing	4.88	3.04	3.03	3.85	4.13	4.30	4.43	4.72

The Four-Source results are again consistent and very stable in the spectrum shape. The final standard deviation values are in the same levels than those from the Rolls-Royce method. Again the results are less than 3 dB error estimation.

Table 5-11. Standard deviation values – Short-cowl (HOT) – Four-Source.

Method / Angle	50	60	70	80	90	100	110	120
FOUR-SOURCE	1.48	1.16	1.79	2.41	2.39	2.51	2.46	2.78

5.5.1. General Routines

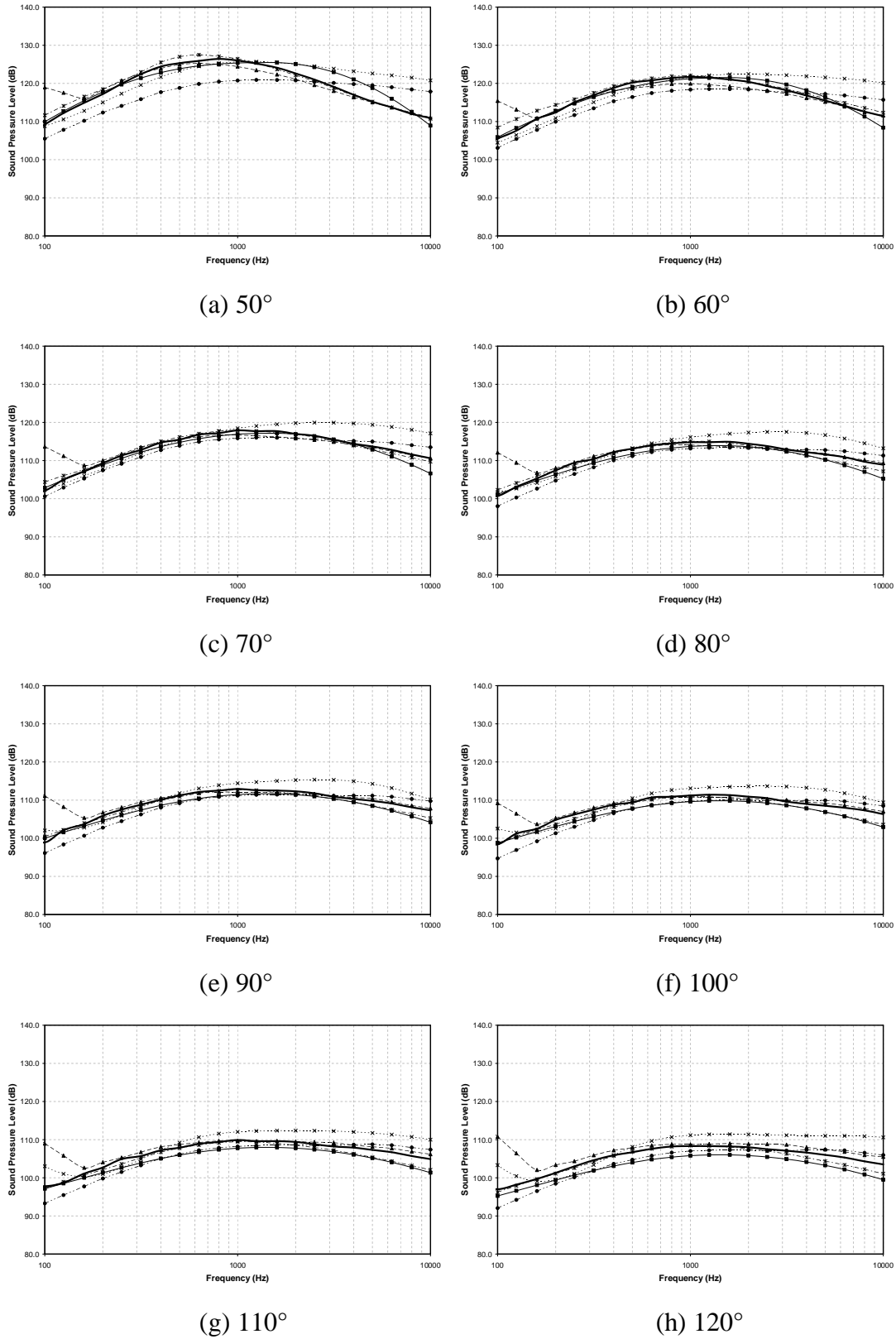
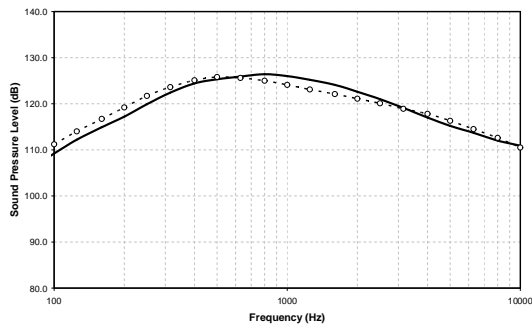


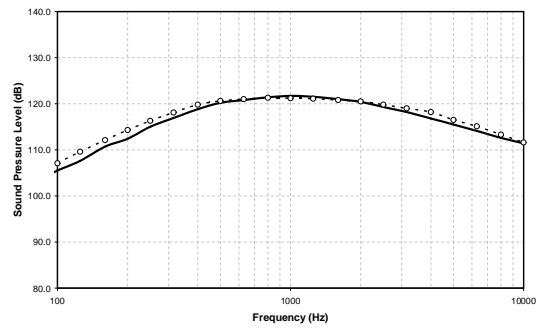
Figure 5-7. Comparison of data with the prediction – Short-cowl (HOT) – General subrotines.

— EXP. DATA —■— SAE 876D —▲— ESDU 01004 ---x--- AIR 1905 - NASA —+— AIR 1905 - ROLLS-ROYCE —◆— AIR 1905 - BOEING

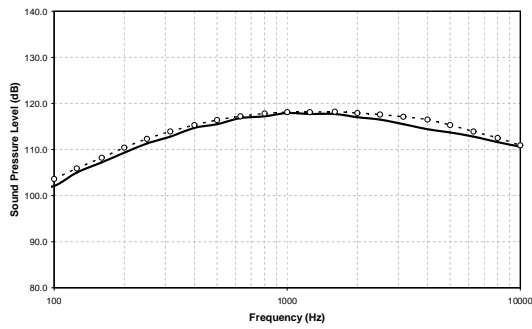
5.5.2. Four-Source Method



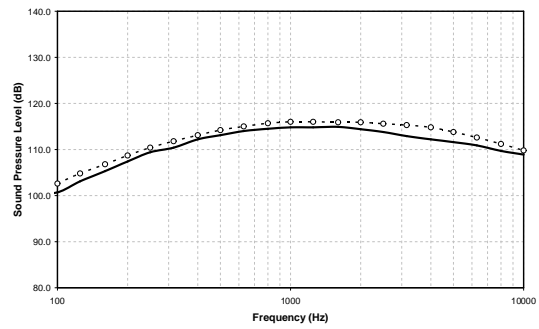
(a) 50°



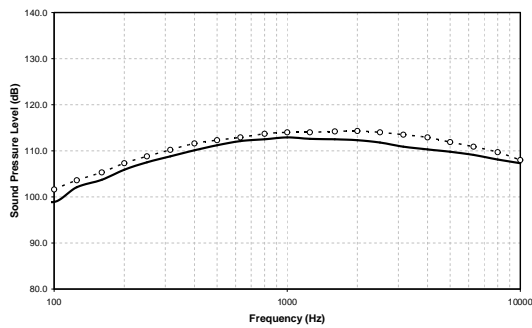
(b) 60°



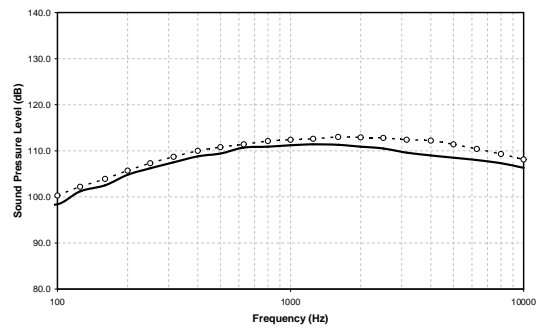
(c) 70°



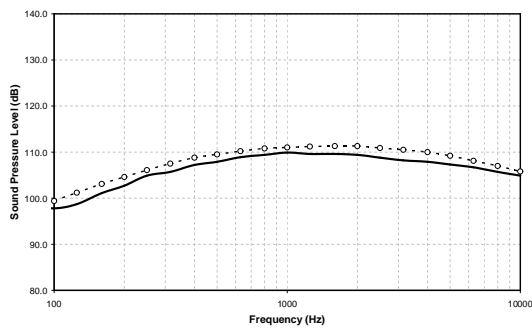
(d) 80°



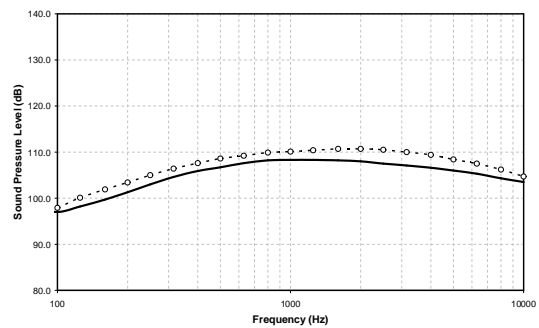
(e) 90°



(f) 100°



(g) 110°



(h) 120°

Figure 5-8. Comparison of data with the prediction – Short-cowl (HOT) – Four-Source.

6. CONCLUDING REMARKS

The main contribution of this work was to provide a general overview of the semi-empirical methods available for noise prediction of dual-stream (coaxial) jets. The most common methods currently available in the literature were implemented and validated against experimental data available at the Institute of Sound and Vibration (ISVR).

A general description of all numerical methods was presented in Chapter 3 and 4 of this document and could be used as a guide for future work in this area. Specifically, Chapter 4 dealt with the Four-Source method, which is a more physically consistent method and most promising for industrial applications.

The main observations from Chapter 5 are summarized and discussed herein as:

- a. The coaxial jet noise spectra are not fairly reproduced numerically for the configurations investigated, when considering standard routines. These traditional methods are within 1 and 5 dB away from the experimental data.
- b. There is no trend in the results, among the standard subroutines, in order to confirm a best one for use as reference. The best results came from SAE AIR 1905 (Rolls-Royce) and ESDU 01004, although the last method presented a series of interpolation problems.
- c. All the standard routines are not completely able to take into account the effect of a short-cowl configuration in a coaxial flow. Although the results are still below 3 or 5 dB (for the worst cases) this effect should be

considered for modern engine exhaust systems.

- d. The Four-Source method provided satisfactory predicted noise levels for both isothermal and hot coplanar coaxial jets, with standard variation not more than 3 dB, for the second case, respectively.
- e. All the spectra shapes from the Four-Source method were very consistent with the experimental data. In terms of noise levels, all values were within 3 dB of data.
- f. Except for extra-corrections needed for the Four-Source method in terms of short-cowl's geometry, the method appears to be reliable for selection as a reference for industrial application. In contrast to the other traditional methods, the Four-Source provided very steady and accurate results.

A next step towards making the Four-Source method more general, would be the extension of the method to take into account short-cowl nozzle configurations. It is worth mentioning that the corrections involved herein are in the order of less than 3 dB, which probably will require extensive experimental work in order to determine the effect of variations in the primary nozzle extent and plugs in the exhaust system.

7. REFERENCES

- [1] FISHER, M. J., PRESTON G. A., BRYCE, W. D., **A modelling of the Noise from Coaxial Jets, Part 1: with unheated primary flow.** Journal of Sound and Vibration 209 (1998) 385-403.
- [2] FISHER, M. J., PRESTON G. A., Mead, C. J., **A modelling of the Noise from Coaxial Jets, Part 2: with heated primary flow.** Journal of Sound and Vibration 209 (1998) 405-417.
- [3] SAE, Society of Automotive Engineers; **Gas Turbine Exhaust Noise Prediction.** Aerospace Recommended Practice ARP-876D. 1994.
- [4] ESDU, Engineering Science Data Unit; **Computer Based Estimation Procedure for Coaxial Jet Noise.** Data Item 01004. 2001.
- [5] SAE, Society of Automotive Engineers; **Gas Turbine Coaxial Exhaust Flow Noise Prediction.** Aerospace Information Report AIR-1905. 1985.
- [6] KO, N. W. M, KWAN, A. S. H., **The Initial Region of Subsonic Coaxial Jets.** Journal of Fluid Mechanics, 73 (2) (1975), 305-332.
- [7] STRANGE, P. J. R., PODMORE, G., FISHER, M. J., TESTER, B. J., **Coaxial Jet Noise Source Distributions.** AIAA/NASA 9th Aeroacoustics Conference, paper no. AIAA-84-2361.
- [8] LIGHTHILL, M.J.; **On Sound Generated Aerodynamically. I - General Theory.** Proceedings of the Royal Society of London, Series A, Mathematical and Physical Sciences, vol 211, no. 1107, p. 564-587. March 1952.
- [9] TANNA, H. K., MORRIS, P. J., **The Noise from Normal-velocity-profile Coannular Jets.** Journal of Sound and Vibration, 98(2) (1985) 213-234.

- [10] MORFEY, C. L., **Amplification of Aerodynamic Noise by Convected Flow Inhomogeneities.** *Jornal of Sound and Vibration*, 28 (1973) 563-585.